

INTRODUCTION

Developmental language disorder is an unexpected and persistent impairment in language ability despite adequate opportunity and intelligence (Newbury et al., 2010). This condition affects between 5-8% of children and is a lifelong disability with an increased risk of behavioural disorders, social problems and literacy deficits.

Calcium-transporting ATPase 2C2 (ATP2C2) is localised in chromosome 16q and the G>A missense mutation is in exon 3. It encodes for SPCA2, a transmembrane protein involved in the transport of Ca²⁺ and Mn²⁺ that is highly expressed in the brain (Xiang et al., 2005).

AIMS

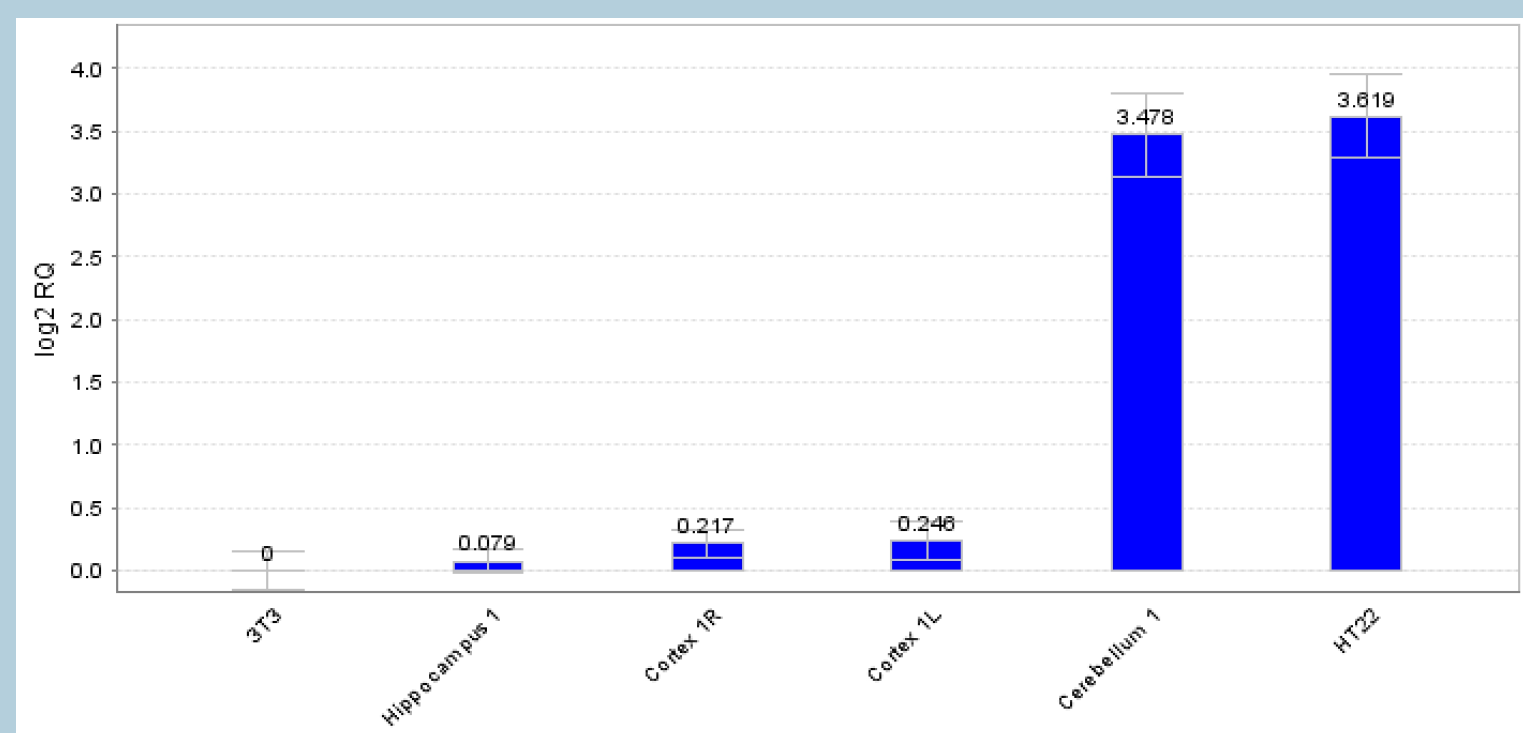
- Evaluate ATP2C2 gene expression in human and mouse cell lines
- Assess post-translational modification in human cell lines
- Show subcellular localisation of SPCA2
- Perform ATP2C2 gene silencing using siRNA
- Optimise primer pair concentration and validate efficiency
- Calculate the frequency of rs78887288 in individuals selected for reading impairment

RESULTS

mRNA EXPRESSION

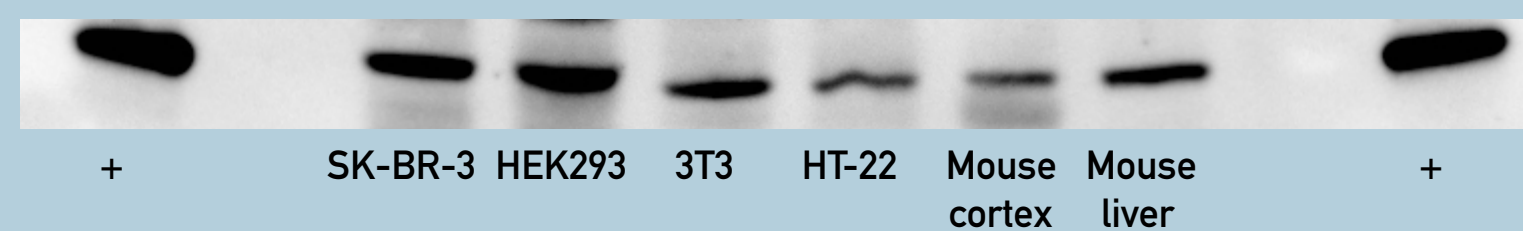


Amplification by PCR of ATP2C2 cDNA revealed that ATP2C2 is expressed in SK-BR-3, MCF-7, HEK293, SH-SY5Y, differentiated SH-SY5Y, HeLa and neural stem cells (141 bp).



Quantitative RT-PCR showed that ATP2C2 is highly expressed in mouse cerebellum and HT-22, an immortalised mouse hippocampal neuronal cell line.

PROTEIN EXPRESSION

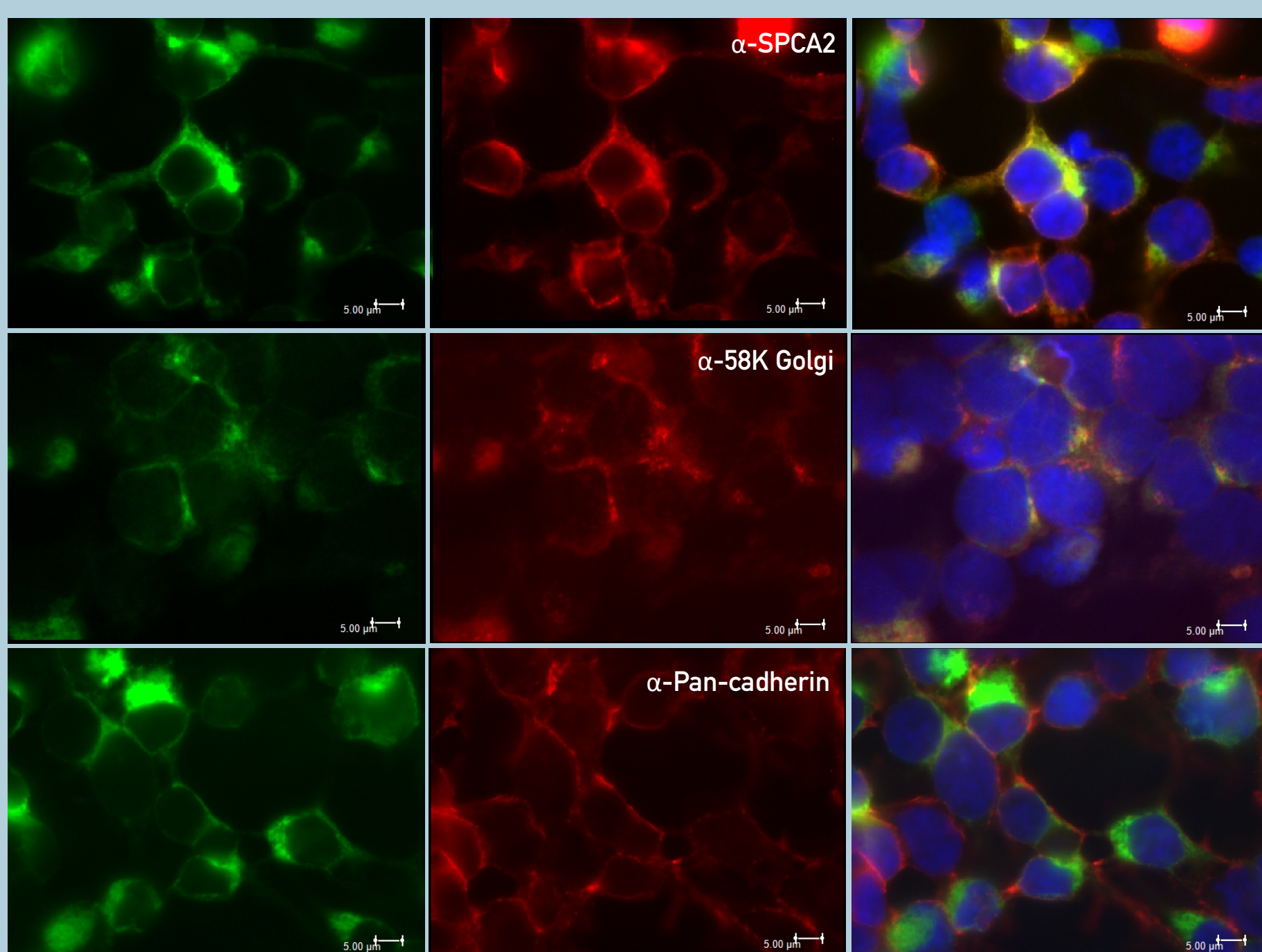


Western blot of SPCA2 showed bands of two different sizes, a slightly larger band for human cell lines and a smaller band for mouse cell lines, cortex and liver (expected 103 kDa). We speculated that this could have been due to some form of post-translational modification.



After deglycosylation, Western blot showed that the size of the bands did not change. Future plans would include attempting deacetylation, deubiquitination and dephosphorylation.

SUBCELLULAR LOCALISATION



Immunofluorescence of overexpressed SPCA2 in HEK293 cells revealed that the protein localises in the Golgi and plasma membrane.

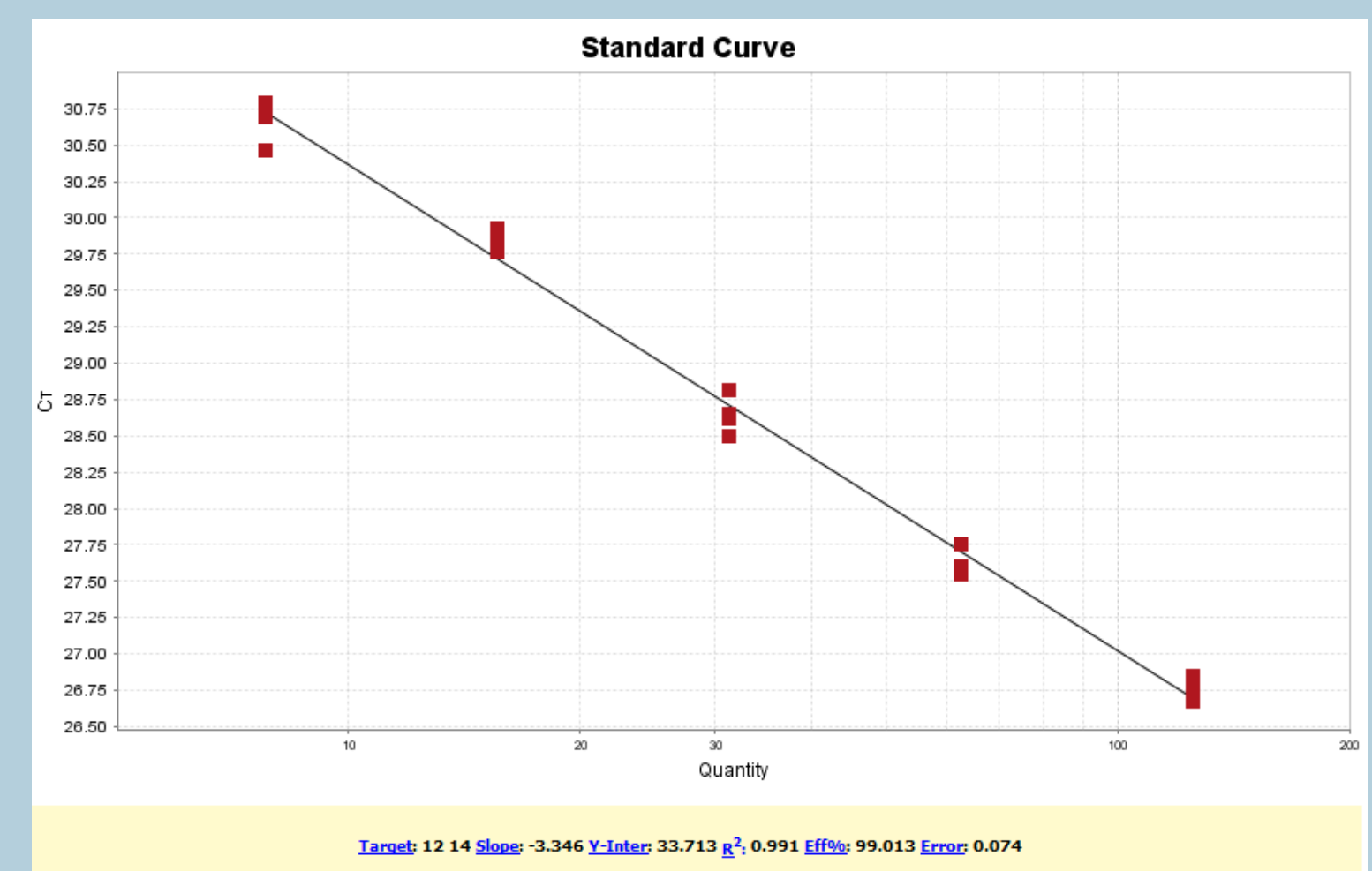
GENE SILENCING

HEK293 cells underwent 3 siRNA transfections.



Western blot verified the silencing of endogenous ATP2C2.

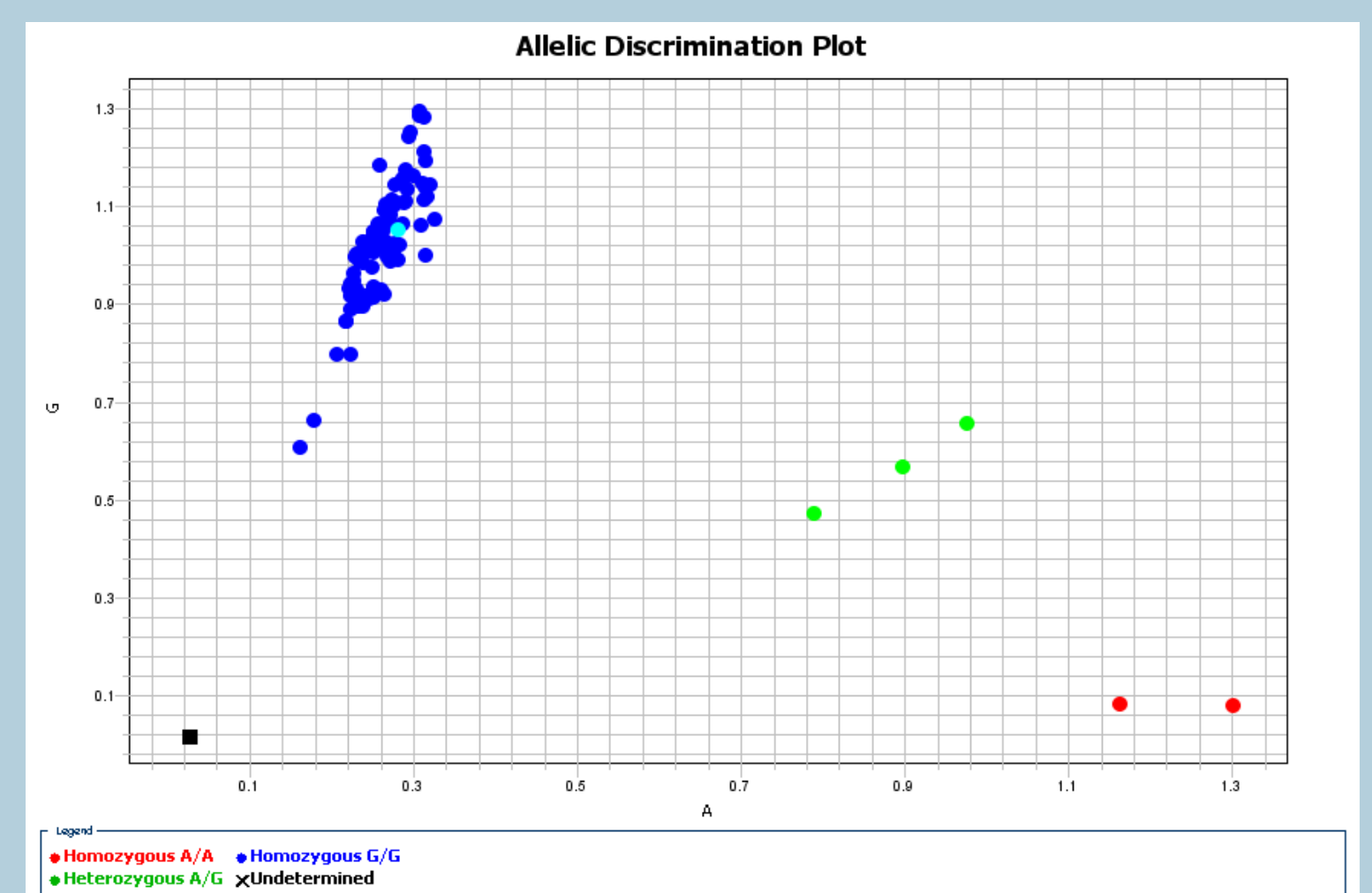
qPCR PRIMER EFFICIENCY



Primer pair concentration was optimised and efficiency validated with a standard curve for HT-22 to minimise non-specific amplification.

HUMAN GENETICS

A large clinical cohort (N=2017) and a control group (N=1867) was screened. DNA was extracted from saliva samples and Taqman SNP genotyping assay run concurrently with a PCR reaction was used to generate a distinguishable product depending on the genotypic status of rs78887288.



Cases filtered to exclude IQ<85 and READ>-1 s.d. from the standardised population mean.

COHORT	STRUCTURE	MINOR ALLELE FREQUENCY
Oxford Family Dyslexia	172 singletons	0.01163
Oxford Cases Dyslexia	289 singletons	0.00346
Aston Dyslexia	45 singletons	0
York	39 singletons	0.04286
Combined	545 singletons	0.008318
Controls	781 singletons	0.00964

Minor allele frequency was found to be higher than the control group in the Oxford Family Dyslexia and York cohorts.

REFERENCES

- 1) Newbury, D. F., Fisher, S. E., Monaco, A. P. (2010). Recent advances in the genetics of language impairment. *BMC Genome Medicine*, 2(1), 6.
- 2) Xiang, M., Mohamalawari, D., Rao, R. (2005). A novel isoform of the secretory pathway Ca²⁺,Mn(2+)-ATPase, hSPCA2, has unusual properties and is expressed in the brain. *Journal of Biological Chemistry*, 280(12), 11608-11614.

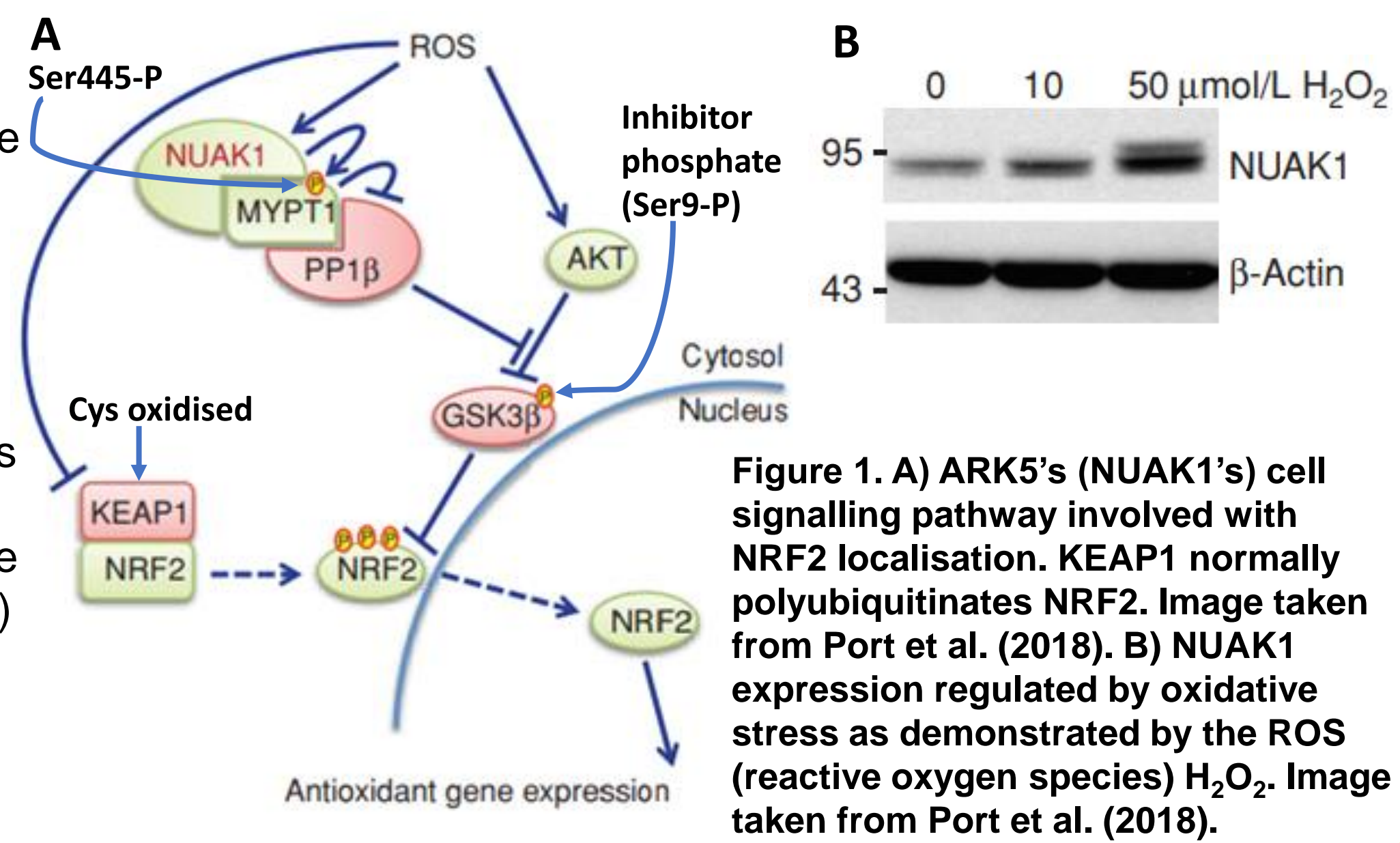
Investigating Mechanisms of Resistance to Oxidative Stress in Renal Cancer

Reynolds lab

Asdaq Raja

Background

Reactive Oxygen Species (ROS e.g. H_2O_2) are by-products of aerobic respiration and have many cellular roles e.g. redox signalling. A few ROSs are harmful but are normally neutralised by cellular antioxidants e.g. glutathione. ROS levels exceeding antioxidant levels can cause widespread damage to DNA, proteins, lipids etc. This is referred to as oxidative damage/stress which usually results in apoptosis but can predispose cells to becoming cancer-like (e.g. increased cell proliferation) or cause cancer (Sosa et al., 2013). Cancer cells have a high metabolic rate resulting in high ROS levels which these cells are resistance to. It is therefore beneficial investigating and preventing different avenues by which cancer cells become resistance to oxidative stress. This project aims to investigate resistance to oxidative stress in renal cancer, starting with ARK5. Port et al. (2018) demonstrated that ARK5 (NUAK1) plays an anti-oxidant role in colorectal cancer cells as ARK5 depletion led to decreased NRF2 (regulates antioxidant proteins, see fig. 1 A) levels and apoptosis (prevented by antioxidant treatment). They also demonstrated ARK5 was positively regulated by H_2O_2 (a ROS) see fig. 1B

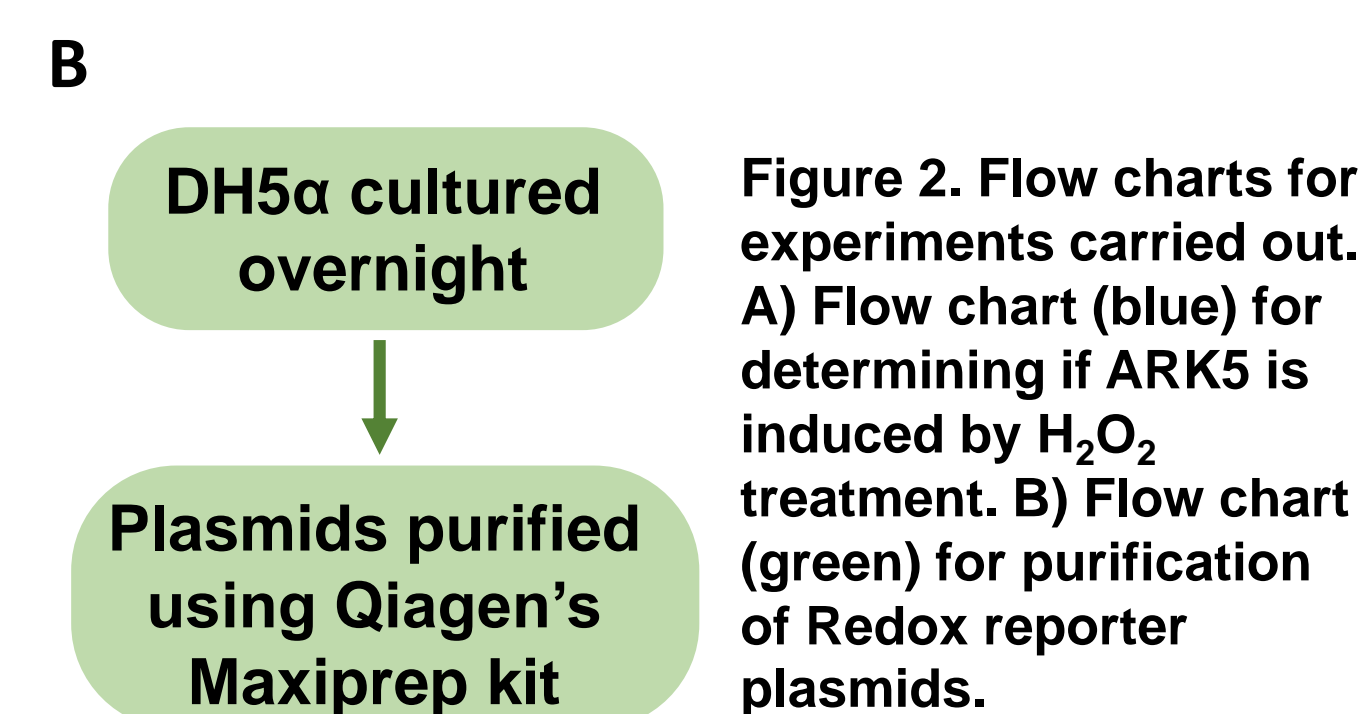
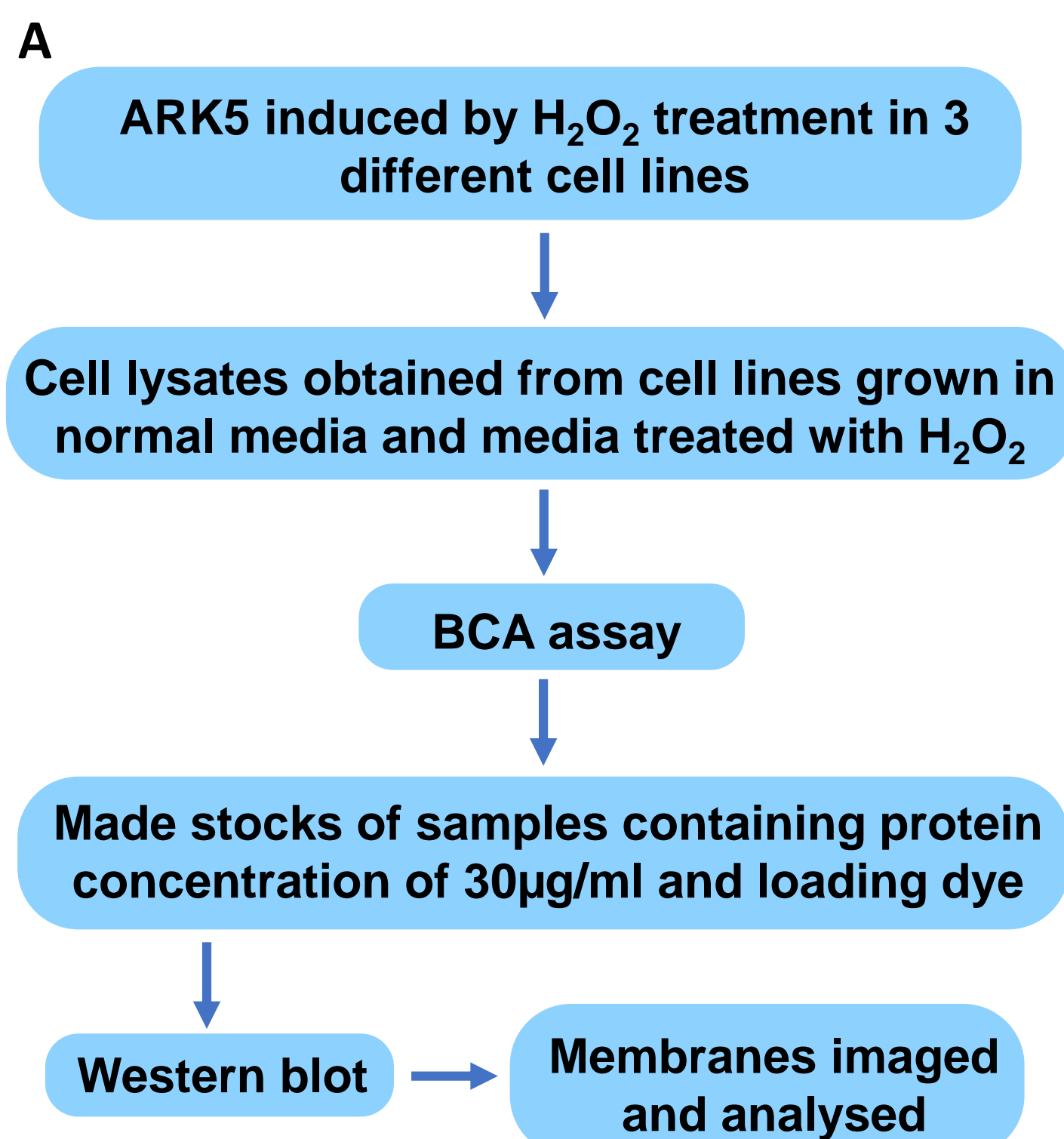


Materials and Methods

Cell lines, media and culture conditions – Cell lines and media:

- 1) **786-O** (renal cell adenocarcinoma) – 500ml RPMI-1640.
- 2) **Caki-1** (renal clear cell carcinoma) – 500ml DMEM with 10% FBS.
- 3) **HK-2** (kidney epithelial papilloma) - - 500ml RPMI-1640.

All media made with 5% FBS and antibiotics penicillin and streptomycin unless stated otherwise. Cultured in 5% CO_2 at 37°C in T-175 flasks with 50mls of the respective media.



Results

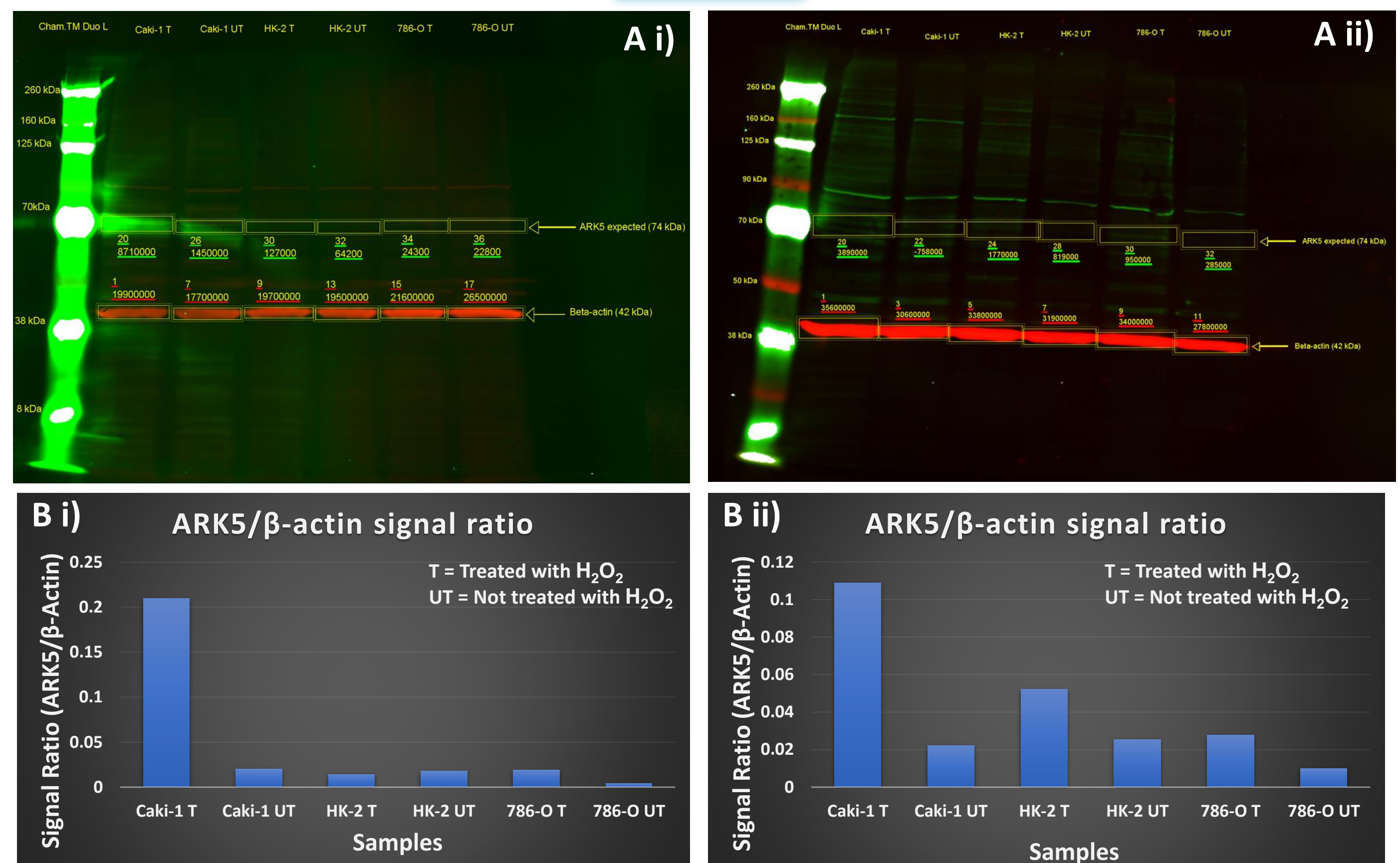


Figure 3. Western blot and signal ratios for ARK5 in cell lines treated with (T) and not treated (UT) with H_2O_2 . A i) and A ii) are western blots for ARK5. B i) and B ii) are the signal ratios calculated for A i) and A ii) respectively. 786-O, Caki-1 and HK2s were plated with either media containing or missing H_2O_2 . Cell lysates obtained for each culture condition and western blots carried out. Signal ratios were calculated from the imaged membrane and represented as a bar chart. Insufficient technical replicates meant a statistical test could not be performed. However, it is clear that ARK5's signal is weak. Perhaps further optimisation steps may be required. Interestingly, fig.3 B ii) may indicate that ARK5 was induced by H_2O_2 , however further technical replicates are required to confirm this observation.

Redox Reporter Plasmids			
Addgene number	Backbone	Insert	Measured Concentration
64975	pLPCX	cyto GRX1-roGFP2	658.1 ng/ μl
64977	pLPCX	Mito GRX1-roGFP2	387.2 ng/ μl
64992	pLPCX	mito roGFP2-Orp1	353.4 ng/ μl
64991	pLPCX	roGFP2-Orp1	297.5 ng/ μl

Table 1. Redox reporter plasmids listed, concentrations and respective addgene number. Plasmids described in detail in Gutscher et al (2008) and (2009) as well as on addgene.

Reporter plasmids in DH5 α purified from overnight culture and concentrations measured are listed in table 1. Plasmids would report degree of oxidative stress in cells under different oxidative conditions..

Discussion

As previously discussed, the western blot revealed weak signals for ARK5 (see. fig 3) however one western blot (see fig. 3 A ii & B ii) did reveal a potential trend that H_2O_2 may induce the expression of ARK5. More technical replicates will need to be performed and the resulting data subject to statistical validation to confirm if the observation was significant. Future experiments would include: 1) Assessing the anti-oxidation defence of renal cancer cells in response to different oxidative stresses using the redox reporter plasmids described previously (see table 1) 2) Exploring additional pathways involved in resistance to oxidative stress. If ARK5 was found to be induced by H_2O_2 treatment, further experiments would need to validate that ARK5 functions as described in Port et al. (2018): 1) Susceptibility of cell lines to oxidative stress after ARK5 inhibition and/or siRNA knockdown 2) NRF2 localisation at different ARK5 levels (immunohistochemistry or immunofluorescence) 3) FRET to evidence that ARK5 is in close association with MYPT1 to build evidence that the same signalling pathway is employed.

References

- Gutscher, M., Pauleau, A., Marty, L., Brach, T., Wabnitz, G., Samstag, Y., Meyer, A. and Dick, T. (2008). Real-time imaging of the intracellular glutathione redox potential. *Nature Methods*, 5(6), pp.553-559.
- Gutscher, M., Sobotta, M., Wabnitz, G., Ballikaya, S., Meyer, A., Samstag, Y. and Dick, T. (2009). Proximity-based Protein Thiol Oxidation by H_2O_2 -scavenging Peroxidases. *Journal of Biological Chemistry*, 284(46), pp.31532-31540.
- Port, J., Muthalagu, N., Raja, M., Ceteci, F., Monteverde, T., Kruspig, B., Hedley, A., Kalna, G., Lilla, S., Neilson, L., Bruccoli, M., Gyuraszova, K., Tait-Mulder, J., Mezna, M., Svambaryte, S., Bryson, A., Sumpton, D., McVie, A., Nixon, C., Drysdale, M., Esumi, H., Murray, G., Sansom, O., Zanivan, S. and Murphy, D. (2018). Colorectal Tumors Require NUA1 for Protection from Oxidative Stress. *Cancer Discovery*, 8(5), pp.632-647.
- Sosa, V., Moliné, T., Somoza, R., Paciucci, R., Kondoh, H. and Lleonart, M. (2013). Oxidative stress and cancer: An overview. *Ageing Research Reviews*, 12(1), pp.376-390.

Parental factors in childhood obesity Health Promotion

Daniel Johnstone

School of Medicine, University of St Andrews

Background

- Childhood obesity is a widely recognised public health problem in the UK, affecting 1 in 3 children aged 10-11 and 1 in 5 children aged 4-5
- The paediatric health problem is known to have many associated possible health consequences, such as poor mental health, asthma, cardiovascular problems, type II diabetes and cancer.
- Parents play an invaluable role in paediatric health promotion, and should be targeted as key agents of change.
- Illness and health problems are viewed in a complex way, especially the way in which parents view their children's health

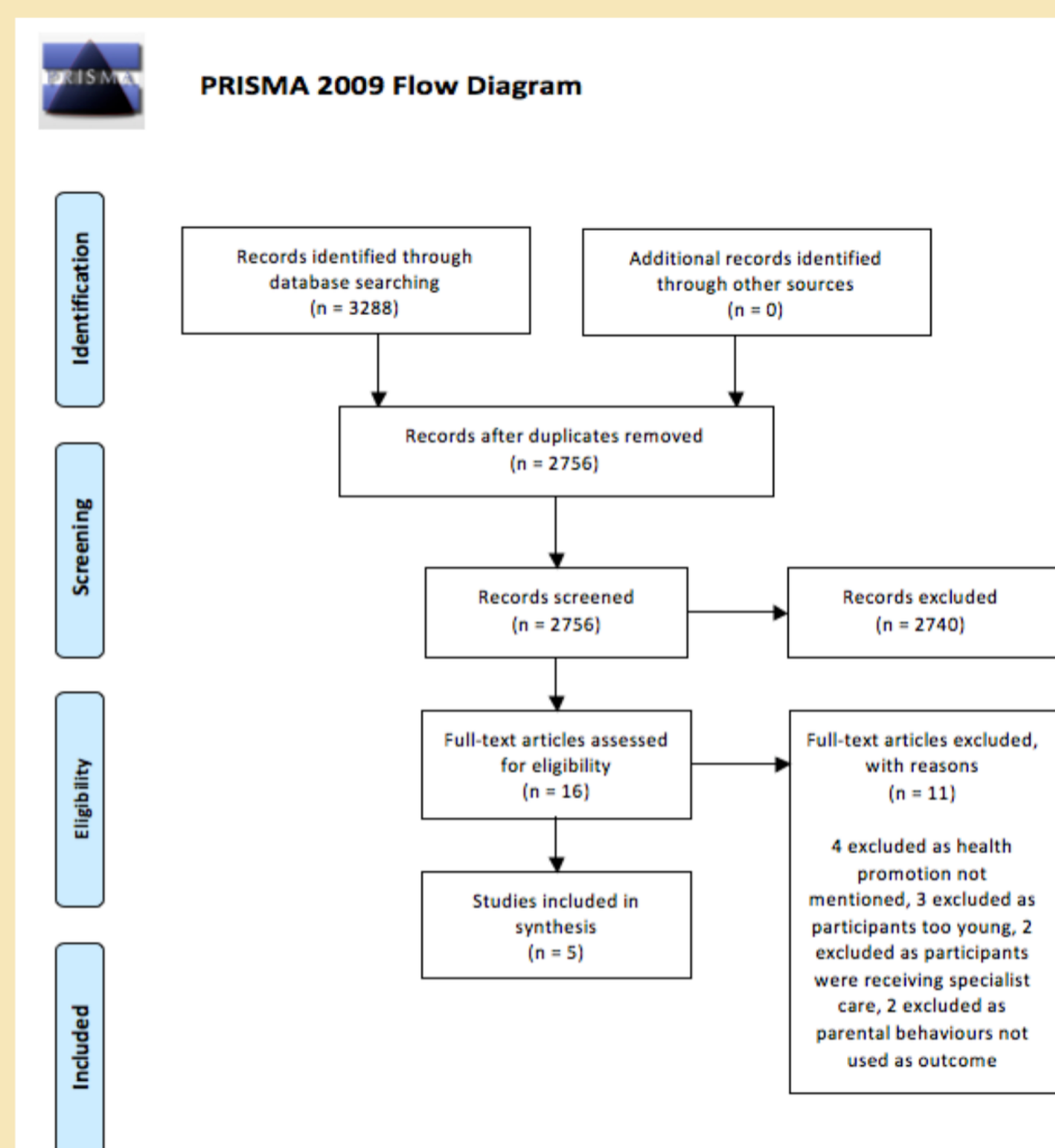


Results

- Of the 5 studies collected, four were conducted in the US, and one conducted in the UK, between 1988-2017. There were four cross-sectional studies and one cohort study reviewed. Four papers all received modest or good quality assurance scores, with the fifth lower scoring paper being from 1988.
- One paper found numerous positive associations between parental perceptions, and their stage of change. with another finding a similar conclusion, showing positive associations of behavioural change and parental recognition of health risks being observed in the unadjusted model. A third paper revealed statistically positive correlations between caregiver support, and perceived risk factors/health complications.
- However, another paper found that parental health beliefs were not significantly associated with weight loss outcome.
- Two papers both agreed that the physician is the key agent of change in child health promotion with respect to obesity.

Methods

- Studies were collected through a comprehensive computerised search of online bibliographic databases (i.e PubMed, EMBASE, PsycInfo and Medline), using advanced search criteria.
- The selection process consisted of duplicate screening, eligibility consideration according to set inclusion/exclusion criteria, and then finally study inclusion. The number of articles excluded at each stage is shown in the PRISMA diagram opposite.
- All selected articles were assessed using STROBE quality assurance checklist



Conclusion

- There are various parental factors which may influence their conformity to positive health behaviours with regards to their child.
- More work is needed with specificity to health promotion to determine whether these factors may have a substantial enough effect to allow mainstream use.



University of
St Andrews

Co-expression of Neuronal signals in Medial Amygdala Kiss neurons

Hyun Wook Kim, Sanya Aggarwal and Javier Tello
School of Medicine, University of St Andrews

Introduction

Kisspeptins (Kiss) are classically known as neuropeptides that control reproductive physiology through actions upon gonadotropin-releasing hormone (GnRH) neurons in the hypothalamus. However, Kiss neurons are also present in the medial amygdala (MeA), which has recently raised interest due to the possible role of linking reproductive behaviour with reproductive endocrine responses. A subset of amygdala Kiss neurons send long-range projections to GnRH neurons in the hypothalamus and specific activation of amygdala Kiss neurons appears to increase social interaction and enhance partner preference in male mice. GnRH neurons are modulated both by neuropeptides such as Kiss but also by neurotransmitters such as glutamate (excitatory) and GABA (inhibitory), which are fundamental for reproductive behaviours. Our experimental aim was to identify the neurotransmitter composition of medial amygdala Kiss neurons to better understand if they function through a complex interplay of neuropeptide and neurotransmitter signalling. The study involved using multiplexed RNAscope *in situ* hybridization and immunohistochemistry on transgenic mouse brains to screen for phenotypic neurotransmitter markers of excitatory (Vglut2) and inhibitory neurons (Vgat), specifically in amygdala Kiss neurons.

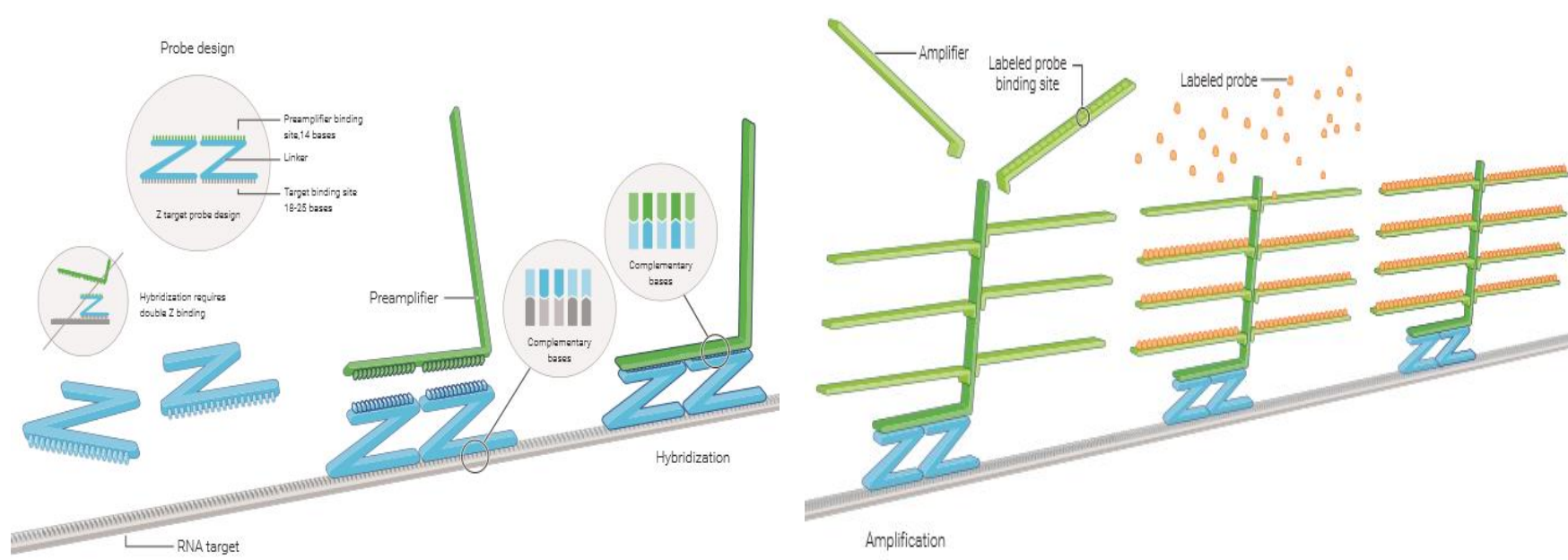


Figure 1 RNA *in situ* hybridization

The complementary probes bind to the target RNA and pre-amplifiers bind to the base of the Z target probes. Multiple amplifiers assemble upon the pre-amplifier and the labeled probes deposit on the amplifiers to display the fluorescent signals *in situ*.

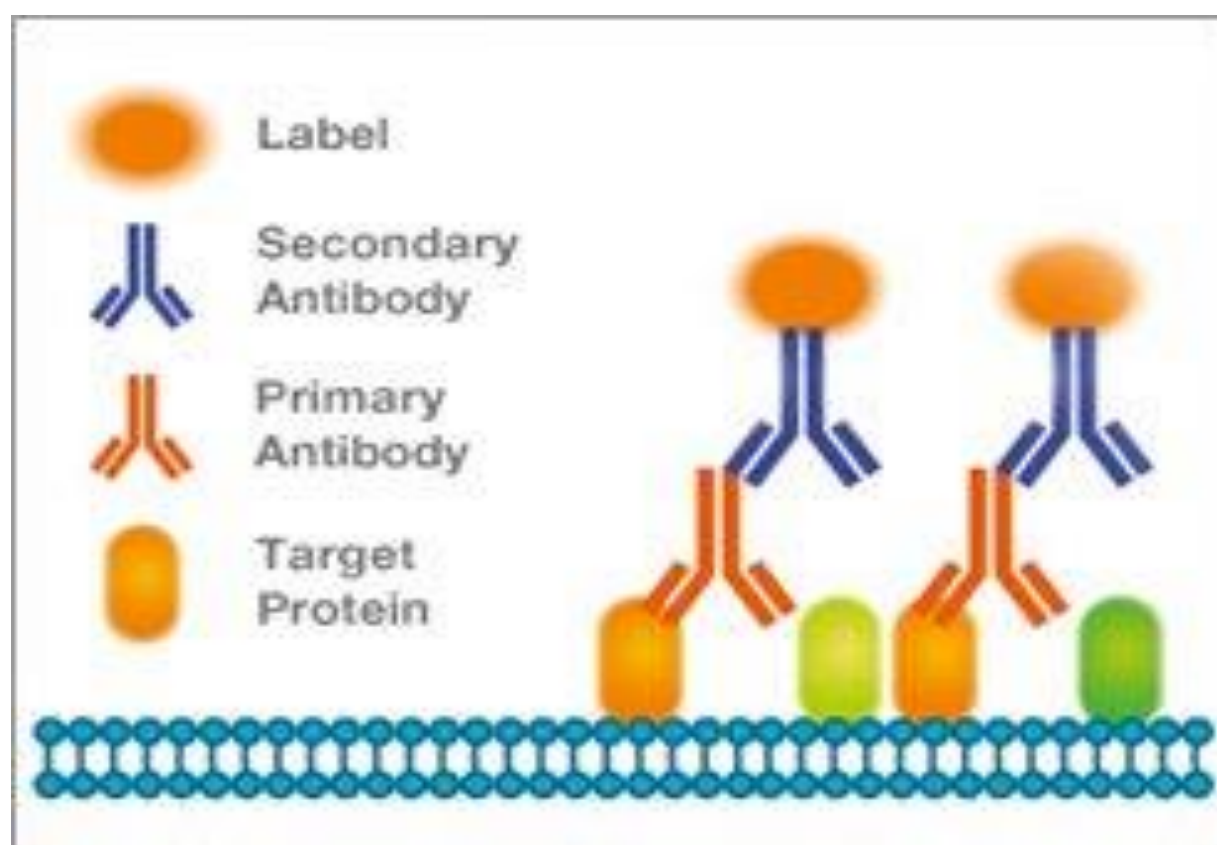


Figure 2 Immunohistochemistry

A primary antibody first detects the antigens of a targeted protein. Secondary antibody that carries a fluorescent protein then attaches to the primary antibody. This allows to locate the targeted protein or amplify the signal if the protein of interest is a weak fluorescent.

Results

The proportion of MeA Kiss neurons that expressed Vgat was 71% whereas that of Vglut2 was 29%. The Kiss neurons that expressed both of the signals were 6%. While most of the Vgat populated in posterodorsal position of the medial amygdala, Vglut2 were more evident in the posteroventral position. Moreover, individual sections from 3 animals at the same Bregma position expressed coherent signals. The negative controls did not show any significant signal.

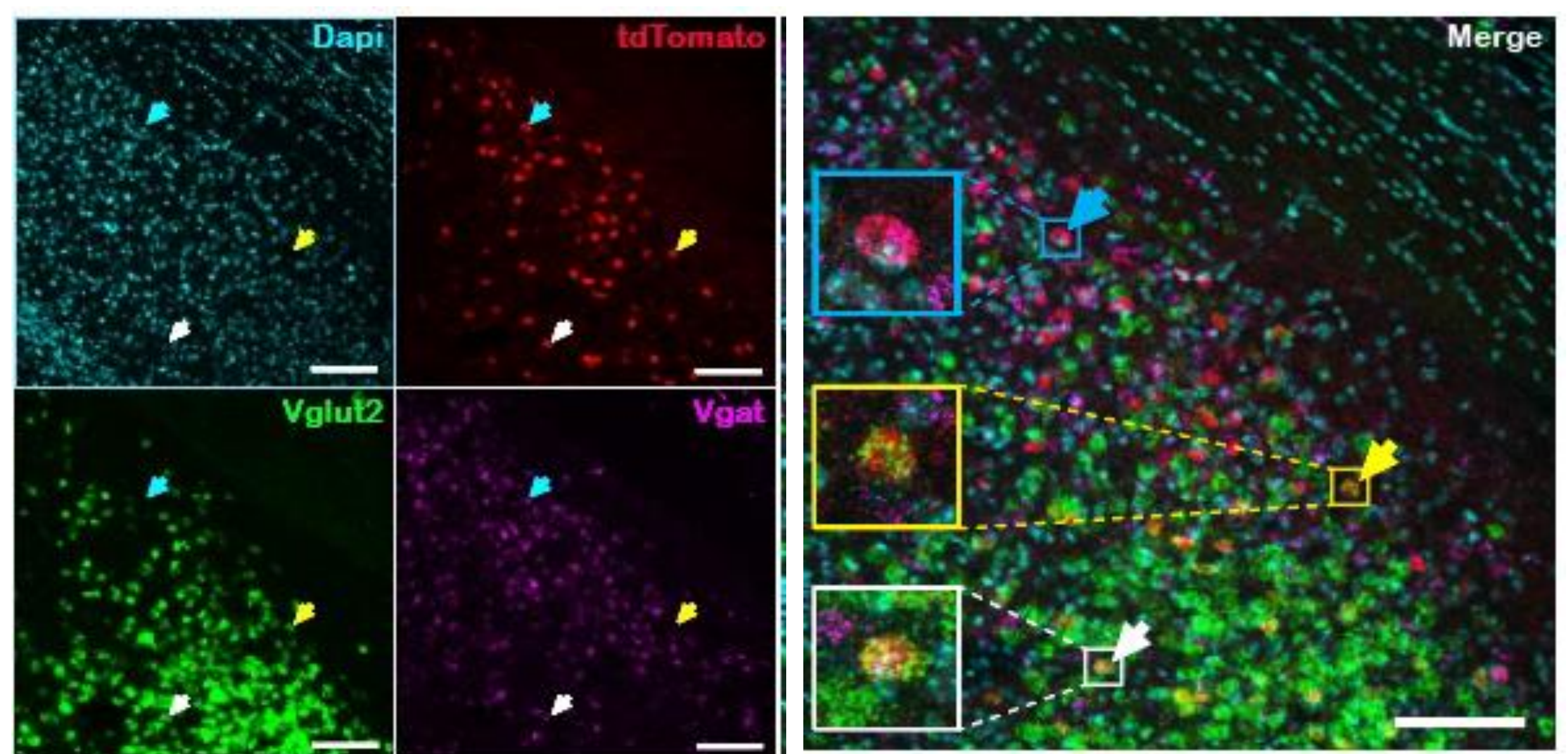


Figure 3 Amygdala Kiss neurons express Vgat and Vglut2 in male mice.

Representative confocal images stacks of dapi stained nuclei (cyan), tdTomato⁺ amygdala Kiss neurons (Red), Vglut2 (green) and Vgat (magenta) in the medial amygdala of male mice; Merged image where the blue box represents a Kiss neuron that expresses Vgat, the yellow box marks a Kiss neuron that expresses Vglut2, and the white box shows a Kiss neuron that expresses both Vgat and Vglut2.

Methods and materials

Three double transgenic Kiss-CreEGFP^{+/+}/Rosa26-LSL-td Tomato^{+/+} adult male mice were used for our study. Double transgenic mice were generated by mating genetically modified Kiss-CreEGFP^{+/+} mice with Rosa26-LSL-td Tomato^{+/+} mice. Their brains were taken and sectioned at 30µm. 3sets of slides each with 2 sections of the brain that contained MeA were prepared for 3 brains respectively. 2 extra sections from one of the mice were used for a positive control and a negative control. The slides were added with 0.6% hydrogen peroxide in methanol and washed with DEPC water to remove endogenous enzymes. The slides were routinely immersed to increasing concentration of ethanol for further cleansing. Hydrophobic barriers were created around the tissues and dried overnight at room temperature. The slides were cleansed with protease. RNA scope procedure was first performed to localise GABA and Glutamate signalling. GABA-ergic neurons were identified by the expression of Slc32a1 mRNA, which encodes the GABA vesicular transporter (Vgat). Glutamatergic neurons were determined by the expression of Slc17a6 mRNA, which encodes the glutamate vesicular transporter (Vglut2). The expression of Kiss neurons labelled with tdTomato (Red Fluorescent Protein) was identified through Immunohistochemistry. Anti-RFP antibody was used as a primary antibody and a donkey anti-rabbit Alexa Fluor 555 was used as a secondary antibody. DAPI was then added to label the nucleus. Images were taken using Leica TCS SP8 confocal-laser scanning microscope.

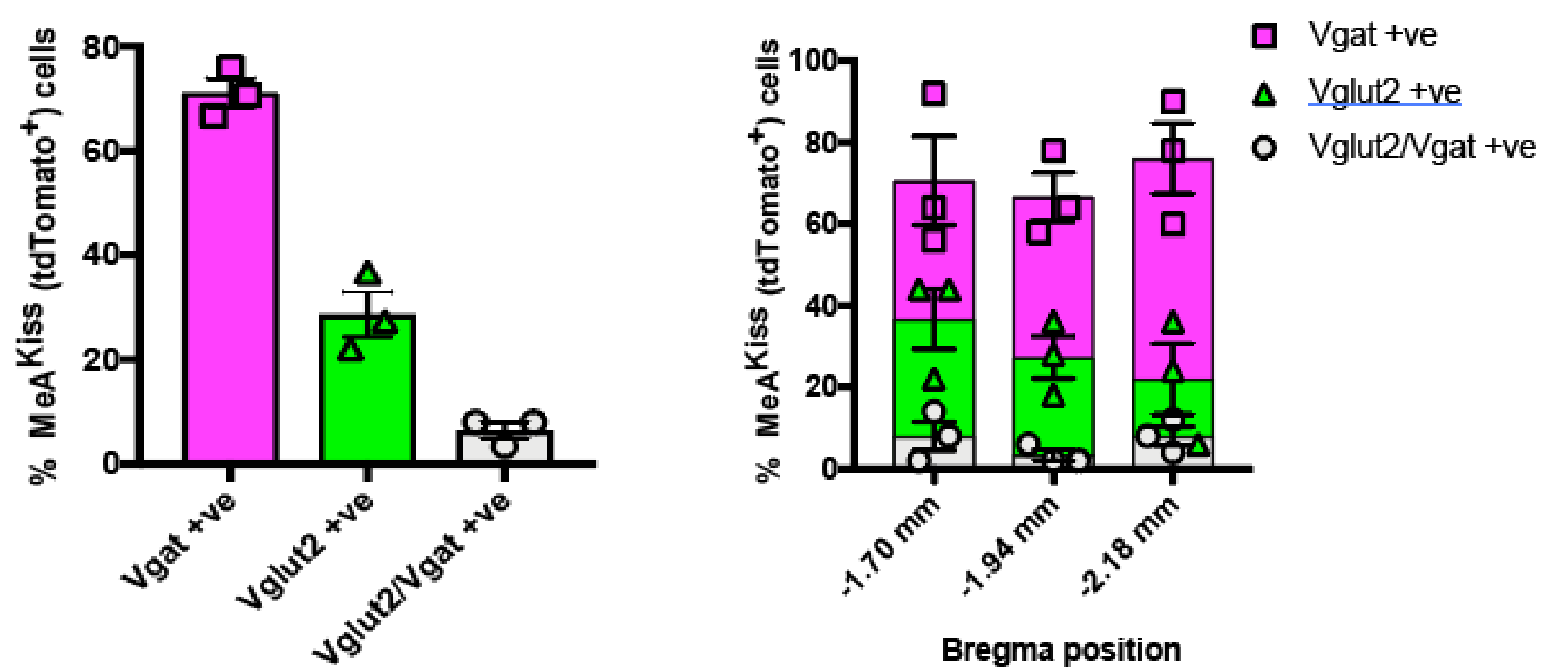


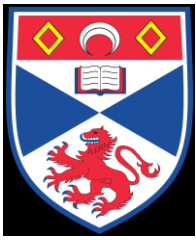
Figure 5 A) The percentage of of amygdala Kiss1 neurons that express Vgat, Vglut2, or both; B) The percentage of amygdala Kiss1 neurons that express Vgat, Vglut2, or both in relation to Bregma position.

Conclusions

We have shown through RNA *in situ* hybridisation and Immunohistochemistry that Kiss neurons in the medial amygdala are a mixed neuronal population, 71% expressing markers for inhibitory neurotransmission (Vgat), 29% expressing markers for excitatory neurotransmission (Vglut2), and 6% expressing both phenotypic markers. We posit that this functional circuitry is mediated by an interplay of neuropeptide and neurotransmitter signalling.

References

- Aggarwal S, Tang C, Sing K, Kim HW, Millar RP, and Tello JA. (under review 2018) *Medial Amygdala Kiss1 neurons mediate female pheromone stimulation of luteizing hormone in male mice*. [Accessed 3 Jul. 2018]
- Bio-Rad. (2018). *Secondary Antibodies* | Bio-Rad. [online] Available at: <https://www.bio-rad-antibodies.com/secondary-antibodiesreagents.html> [Accessed 29 Aug. 2018].
- Acdbio.com. (2018). *How It Works | In Situ Hybridization, RNA-ISH* | ACDBio. [online] Available at: <https://acdbio.com/science/how-it-works> [Accessed 3 Jul. 2018].



The Effects of Calcium Dysregulation on Cardiac Dysfunction in Fabry Disease



L. Kankowski, A. Dorward, G.B. Robertson, S.J. Pitt
School of Medicine, University of St Andrews, St Andrews



Introduction

Fabry disease is a lysosomal storage disorder that results from the build-up of a particular type of fat, called globotriaosylceramide (Gb3), in the body's cells. Fabry disease is strongly associated with an increased risk of cardiac disease including ventricular hypertrophy, heart failure and fatal arrhythmias. However, the mechanism by which Gb3 causes these morphological and functional changes remains unknown(1,2).

Calcium release is a key component of cardiac function. Remodelling of this process has been linked to both mechanical issues in heart failure and electrical dysfunction of cardiac arrhythmias(3). Lysosomes are intracellular organelles thought to be an important intracellular calcium store. NAADP causes the release of calcium through activation of the lysosomal calcium channel named TPC2(4). Recent evidence links the altered NAADP signalling with cardiac arrhythmias.

Hypothesis: Our hypothesis is that, in Fabry disease, altered NAADP signalling results in dysregulated calcium signalling which may contribute to cardiac failure experienced by patients with Fabry disease.

Aims

The aim of this project was to understand how Fabry disease affects NAADP-induced lysosomal calcium release and S/ER calcium stores.

Methods

1. Calcium Imaging

Human fibroblasts isolated from both healthy individuals and individuals with Fabry disease were loaded with 5uM fluo-4 at room temperature for 45mins. Using a Leica DMI8 inverted fluorescent microscope, a series of 250 fluorescent images were taken 2 seconds apart. The change in the fluorescence of 30 cells in each stack was measured following the application of 1uM Endothelin-1 followed by 5uM of ionomycin or 1uM of thapsigargin. To investigate the involvement of NAADP-mediated TPC2 signalling, cells were incubated for 1hr at 37°C with 100uM NED-19 and then exposed to 1uM Endothelin-1 followed by 5uM calcium ionophore ionomycin or 1uM of the SERCA inhibitor thapsigargin. Store levels were assessed by application of 5uM of ionomycin alone in the absence or presence of NED-19.

2. Western Blot

A 96 well plate BCA assay was used to quantify the total protein content of the samples. 10ug of protein from each sample was added to a 12 well gel, using a β actin control and a PageRuler Plus Prestained Protein ladder. The gel was run for 50mins at 200V and transferred for 1hr at 35V. The HRP conjugated secondaries were activated by ECL and imaged using ImageQuant LAS3000.

Acknowledgements

Thank you to The Physiological Society for funding this project.

References

1. Seydelmann N, et al. Fabry disease and the heart. Best Pract Res Clin Endocrinol Metab. 2015;29(2):195–204.
2. Namdar M. Electrocardiographic Changes and Arrhythmia in Fabry Disease. Front Cardiovasc Med [Internet]. 2016;3(March):1–6.
3. Lou Q, et al. Remodelling of Calcium Handling in Human Heart Failure. 2012;740:1145–74.
4. Pitt SJ, et al. TPC2 is a novel NAADP-sensitive Ca²⁺ release channel, operating as a dual sensor of luminal pH and Ca²⁺. J Biol Chem. 2010;285(45):35039–46.

Fabry cells show a reduced ET-1 response and reduced calcium stores

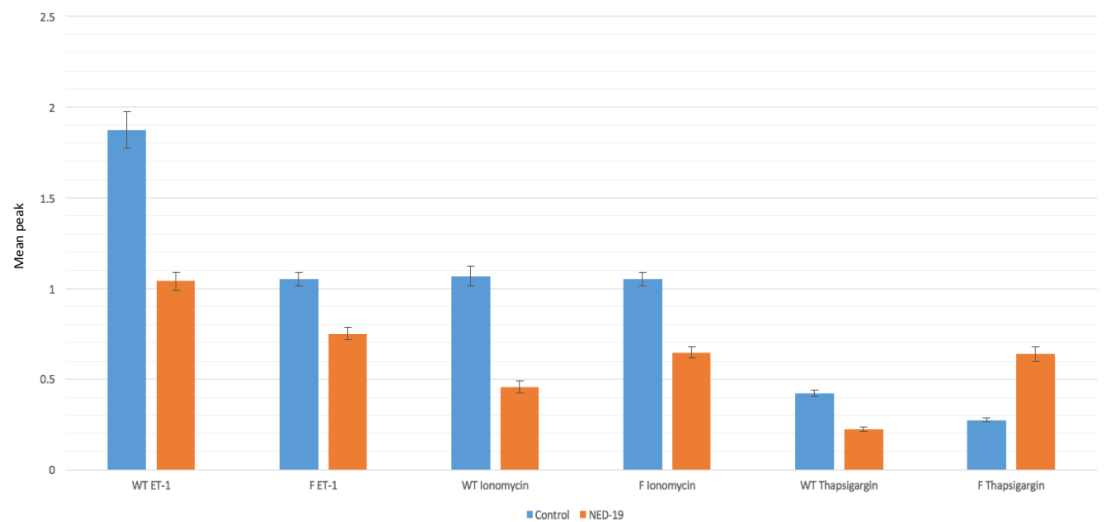


Figure 1: The bar graph shows the average calcium release measured by the mean peak of the change in fluorescence in WT and Fabry cells. Calcium responses following application of 1uM Endothelin-1 in the absence (blue) and presence (orange) of the TPC2 antagonist NED-19. Calcium responses were evoked by 1uM endothelin. Ca²⁺ store levels were assessed by the application of 5uM ionomycin or 1uM thapsigargin.

Calcium responses to ET-1 and thapsigargin were significantly lower in Fabry cells compared to control cells. Fabry cells showed a 41.37% lower response to ET-1 and a 31.8% reduced response to thapsigargin compared to control cells. These differences can be explained by lower intracellular calcium stores in the Fabry cells. However, disparities in either the TPC2 or IP3 receptors may contribute to the reduced ET-1 response. Surprisingly, the responses to ionomycin was not statistically different between the WT and Fabry cells.

Following pre-treatment with 100uM NED-19, Fabry cells showed a 27.84% lower response to ET-1 than WT. Both cell samples show a significant decrease in the calcium response. Wild type cells show an 80.34% decrease in ET-1 response with NED-19, whereas Fabry cells only show a 40.10% decrease. Importantly, treatment of WT cells with NED-19 reduced the calcium response to the same level as that observed for Fabry cells. NED-19 is a non-competitive antagonist of TPC2 and blocks the NAADP pathway of lysosomal calcium release. These data suggest that TPC2 contributes less to the ET-1 mediated Ca²⁺ response in Fabry cells.

TPC2 is upregulated in Fabry cells, but its function may be inhibited

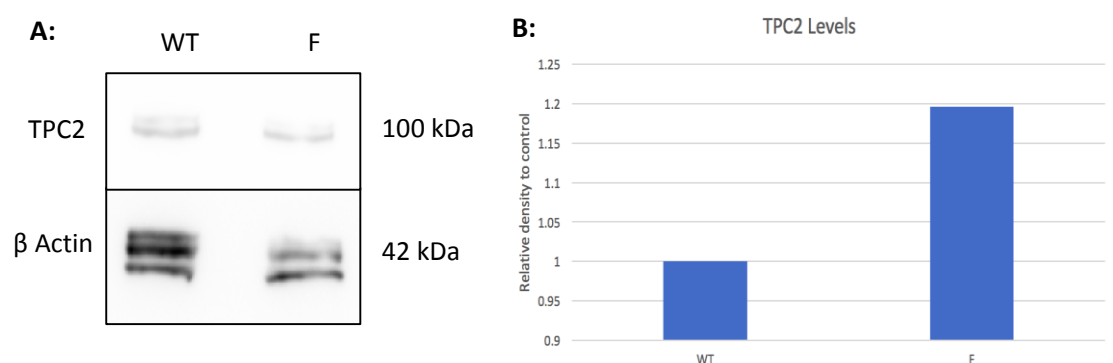


Figure 2: A – Western Blot for TPC2. WT=Wild Type cells F=Fabry cells. B – Graph to show the relative expression of TPC2 in WT and Fabry cells relative to β actin control. Fabry cells showed a 19.6% increase in TPC2 density compared to wild type cells.

Conclusion

This study provides evidence that intracellular calcium remodelling occurs in Fabry disease, which alters intracellular Ca²⁺ dynamics and cell function. Our data suggests that TPC2 receptor expression is elevated in Fabry disease but surprisingly NAADP stimulated lysosomal calcium release is reduced. These data suggest that TPC2 function is impaired in Fabry disease.

Cardiac disease, in particular heart failure of fatal arrhythmias, are recognised as common end-organ complications of Fabry disease. Although further research is required to fully understand the mechanism by which heart failure and arrhythmias develop, the outputs of this work will help define the molecular mechanisms that link Fabry with impaired Ca²⁺ signalling and may highlight the lysosomal signalling pathway as a potential new drug target in the treatment against cardiopathologies associated with Fabry disease.

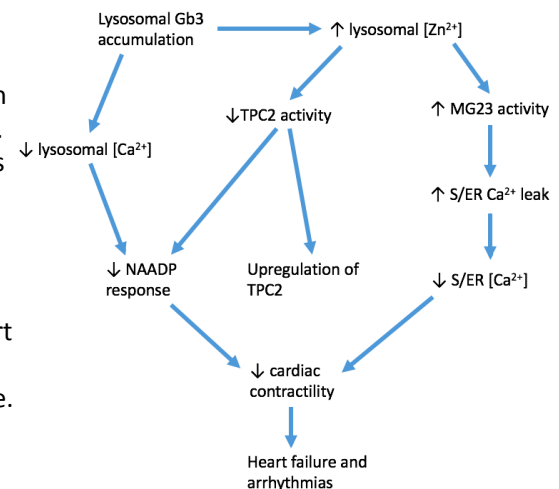


Figure 3: Proposed model of the mechanism of cardiac dysfunction in Fabry disease.



Introduction

Parkinson's disease (PD) is the second most common neurodegenerative disease affecting 10 million people worldwide. A key protein linked to the aetiology of the disorder is alpha-synuclein for which misfolding is linked to the pathogenesis. One proposed mode of transfer between cells of the brain is via exosomes that are nanovesicles released from multivesicular endosomes. Trafficking in the endosome system thus has potential to modulate exosome production and affect the transfer of misfolded alpha-synuclein. One gene implicated in late-onset familial PD is vacuolar protein sorting-35 (VPS35). VPS35 is a component of the retromer complex involved in retrograde trafficking from endosome to the Golgi apparatus. Our hypothesis is that knockdown of VPS35 will enhance or modulate exosome biogenesis and augment the release of exosome-associated alpha-synuclein from cells. We suggest exosomes from VPS35 knockdown cells will be more potent in transfer of alpha-synuclein between cells.

Objectives

1. To establish VPS35 knockdown in undifferentiated SH-SY5Y neuronal cells
2. To measure the levels of multi-vesicular endosomes and their internal vesicles in intact SH-SY5Y cells using electron microscopy (EM), and assess the impact on trafficking through the endosome system using established immunofluorescence markers
3. To investigate the effect of VPS35 knockdown on the fate of endocytosed alpha-synuclein with focus on multi-vesicular bodies (MVBs)

Methods

Undifferentiated SH-SY5Y cells were cultured in combination with knockdown using siRNA and scrambled sequences as controls (Thermo-Fisher). After knockdown, cells were analyzed using immunoblotting and also fixed for immunofluorescence (IF/confocal microscopy) and conventional section-based TEM. Endosome markers (EEA1 and LAMP1) were localized by IF, and endosomal structures including MVBs were quantified using thin-section EM. From these samples, supernatants were collected and 2µl assayed for nanovesicles using the EM-based Nanocount method. This tested whether the output of exosomes was affected by VPS35. We then incubated SH-SY5Y cells with 2µg/ml of exogenous alpha-synuclein for 4hrs. Using IF and immuno-EM, we assessed the distribution and concentration within the endosomal system and compared the effects of VPS35 knockdown on these parameters.

Results

Achieving Knockdown of VPS35: Knockdown was validated by using western blot (WB) and IF methods.

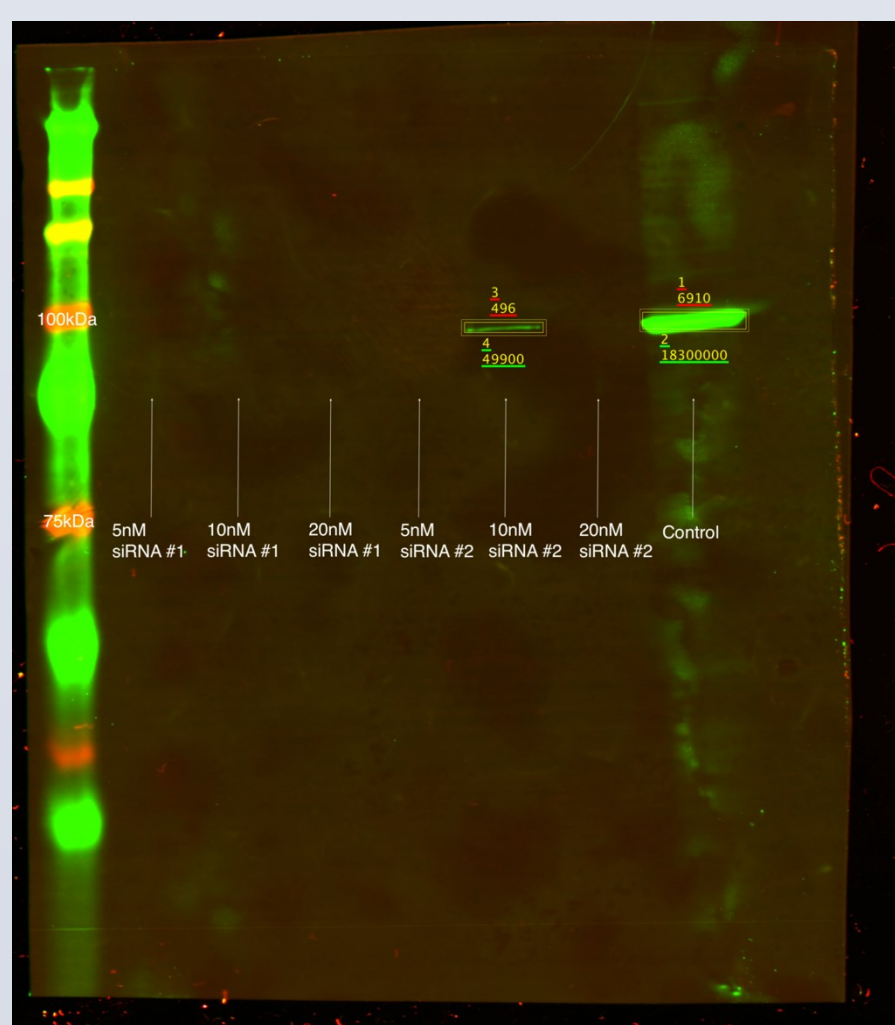


Figure 1: Samples with equal protein content were analysed by Western blotting. Using polyclonal antibodies raised against VPS35, all siRNAs caused marked reduction in expression of VPS35.

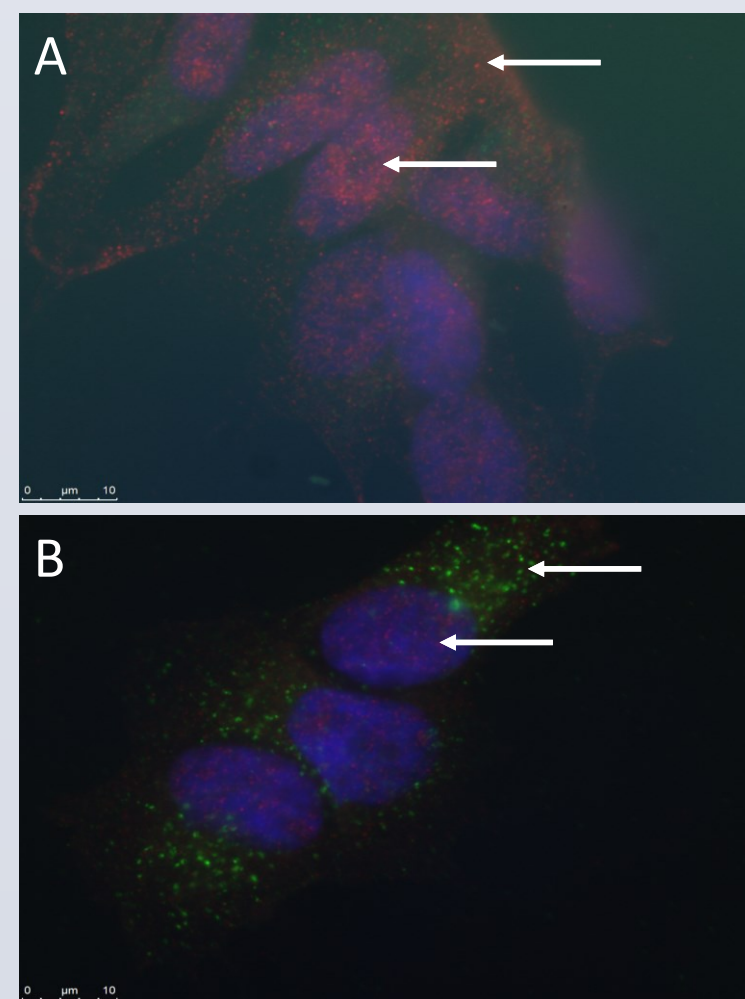


Figure 2: Double IF staining of VPS35 (red) and EEA1 (green) in SH-SY5Y cells. In untreated controls (A), staining for VPS35 is seen both in the nucleus and cytoplasm, while EEA1 is seen in the cytoplasm. On knockdown (B), staining for VPS35 is reduced while EEA1 is increased and localized around the juxtannuclear region of the cells.

EM of Endosomal Structures

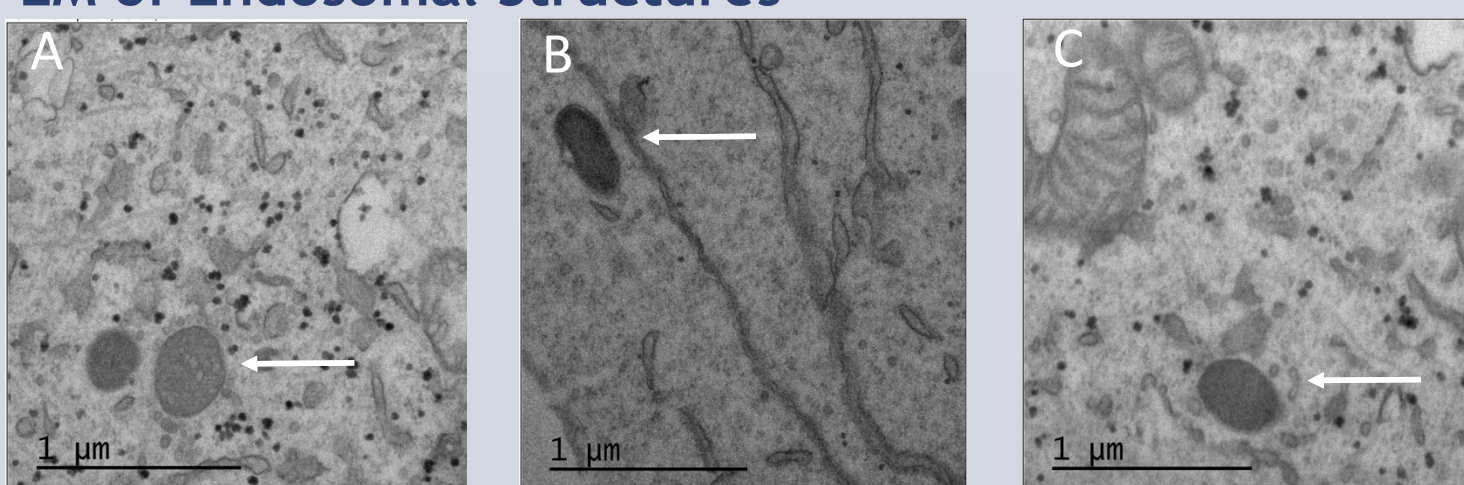


Figure 3: (A) Multivesicular body (B) Multilamellar body (C) Homogenous body

We started to use EM to count the number of endosomal structures and their vesicular (exosomal) content in SH-SY5Y control cells, and then planned to observe if there was a change with VPS35 knockdown. MVBs (Figure 3A) are late endosomal structures containing internal membrane-bound vesicles. Multilamellar bodies (MLBs) (Figure 3B) are single membrane endosomal structures containing intraluminal membranes. Homogenous bodies (HBs) (Figure 3C) are endosomal structures with unified density throughout and no visible internal vesicles. 30 MVBs, 55 MLBs, and 45 HBs were counted using a stereological scanning approach establishing the method for further investigations of VPS35 knockdown. Interestingly, fewer MVBs were observed than expected.

Immunofluorescence Study

In control cells, immunofluorescence signal for VPS35 was found in punctate structures in both the cytoplasm and nucleus. As found in previous publications there was little overlap of the VPS35 with the EEA1 and LAMP1 markers. Significantly, the VPS35 signal was almost abolished after knockdown establishing the specificity of the antibody in IF. After knockdown the extent and distribution of the IF signal of EEA1 and LAMP1 markers changed in the cells. These signals not only increased in size and number, but were also more focused around the juxtannuclear region indicating strong changes in the endocytic pathway.

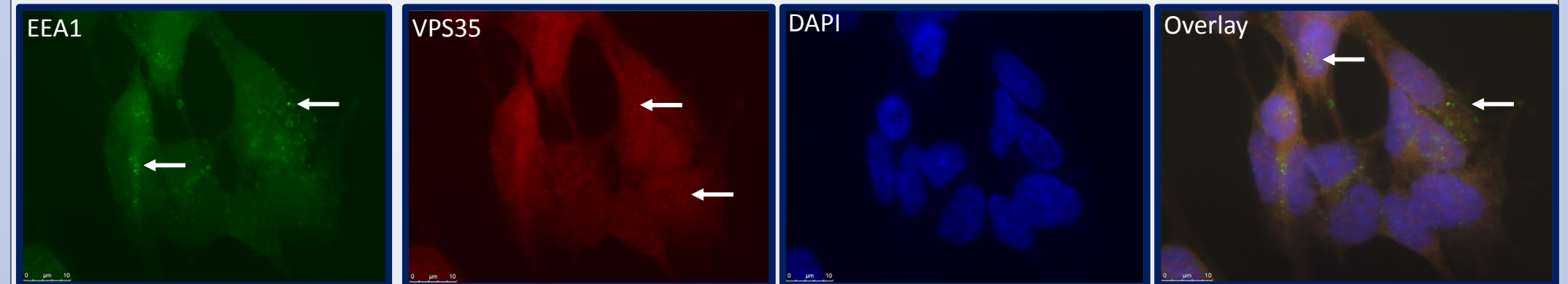


Figure 4: EEA1 Control, 100x. EEA1 signal is scattered throughout the cells. VPS35 signal is present (arrows). There is little overlap of VPS35 with EEA1.

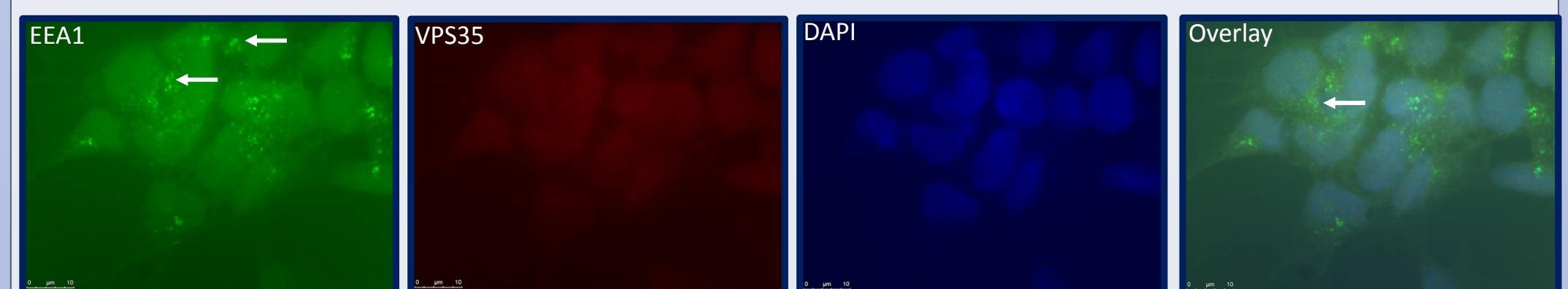


Figure 5: EEA1 Knockdown, 100x. EEA1 signal (arrows) is greater and more focused around the juxtannuclear region of the cell. VPS35 signal is greatly reduced.

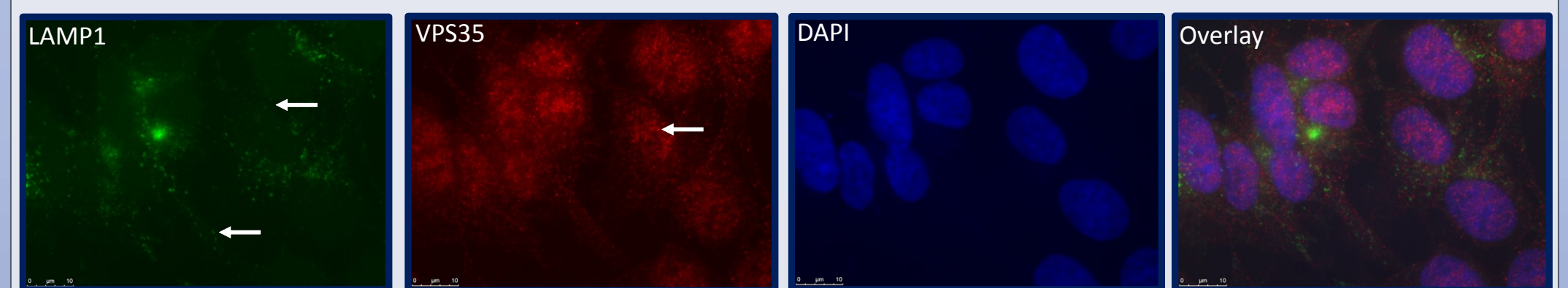


Figure 6: LAMP1 Control, 100x. LAMP1 signal (arrows) is weaker and scattered throughout the cells. VPS35 signal (arrow) is very strong. There is little overlap of VPS35 with LAMP1.

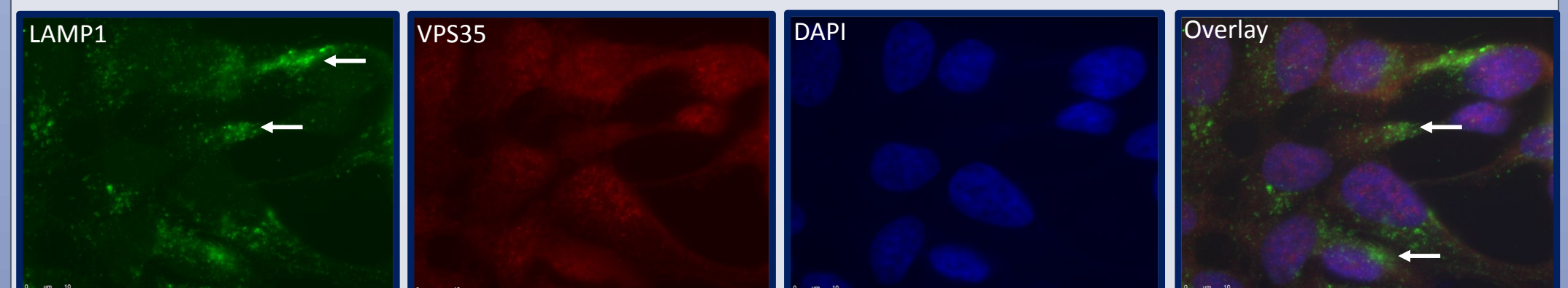


Figure 7: LAMP1 Knockdown, 100x. LAMP1 signal (arrows) is greater and more focused around the juxtannuclear region. VPS35 signal is greatly reduced.

Conclusion

Our hypothesis proved valid. With knockdown of VPS35 there's a trend of increased endosomal size based on increased signal from EEA1 and LAMP1 endosomal markers. The focused signal around the juxtannuclear region of the cells could indicate that the endocytic recycling pathway is blocked. For instance, perhaps recycling of endosomes back to the Golgi apparatus is not occurring, causing lysosomes containing increased amounts of aSN, to expand in the knockdown experiments and a larger signal to be seen. As planned in our experimental design, in future studies, the quantification of the number and size of MVBs and their vesicles should be performed, as well as that for extracellular vesicles. Future studies specifically measuring levels of alpha-synuclein as well as using immuno-EM to quantify endosomal changes should be performed. It would also be interesting to perform these experiments in differentiated SH-SY5Y cells to observe any changes.

Acknowledgements

Many thanks to the Lucocq Lab and to the University of St Andrews School of Medicine for hosting this Wellcome trust funded Vacational Scholarship.

References

1. Chistiakov DA, Chistiakov AA. (2017) α -Synuclein-carrying extracellular vesicles in Parkinson's disease: deadly transmitters. *Acta Neurol Belg.* 117:43.
2. Domingo A, Klein C. (2018) Chapter 14 - Genetics of Parkinson's Disease. *Neurogenetics.* 147:211-227.
3. Gao Y, Wilson GR, Stephenson SEM, Bozaoglu K, Farrer MJ, Lockhart PJ. (2018) The emerging role of Rab GTPases in the pathogenesis of Parkinson's disease. *Mov Disord.* [Epub ahead of print].
4. Hacker C, Asadi J, Pilotas C, Ferguson S, Sherry L, Marius P, Tello J, Jackson D, Naismith J, Lucocq JM. (2016) Nanoparticle suspensions enclosed in methylcellulose: a new approach for quantifying nanoparticles in transmission electron microscopy. *Sci Rep.* 6:25275.
5. Jiang P, Gan M, Yen S, McLean PJ, Dickson DW. (2017) Impaired end-lysosomal membrane integrity accelerates the seeding progression of α -synuclein aggregates. *Sci Rep.* 7:7690.
6. Miura E, Hasegawa T, Konno M, Suzuki M, Sugeno N, Fujikake N, Geisler S, Tabuchi M, Oshima R, Kikuchi A, Baba T, Wada K, Nagar Y, Takeda A, Aoki M. (2014) VPS35 dysfunction impairs lysosomal degradation of α -synuclein and exacerbates neurotoxicity in a *Drosophila* model of Parkinson's disease. *Neurobiol Dis.* 71:1-13.
7. Tang FL, Liu W, Hu JX, Erion JR, Ye J, Mei L, Xiong WC. (2015) VPS35 Deficiency or Mutation Causes Dopaminergic Neuronal Loss by Impairing Mitochondrial Fusion and Function. *Cell Rep.* 1210:1631-43.
8. Temkin P, Morishita W, Goswami D, Arendt K, Chen L, Malenka R. (2017) The Retromer Supports AMPA Receptor Trafficking During LTP. *Neuron.* 941:74-82.
9. Shipley MM, Mangold CA, Szpara ML. (2016) Differentiation of the SH-SY5Y Human Neuroblastoma Cell Line. *Jove.* 108.

ELUCIDATING THE ROLE OF DUSP6 IN COLORECTAL CARCINOGENESIS

Ganesanathan S.¹, Williams H.¹, Harrison D.¹

¹ University of St Andrews, School of Medicine, St Andrews, United Kingdom



University of St Andrews

Introduction and Aims

- Cytoplasmic Dual Specificity Phosphatase 6 (DUSP6) serves to negatively regulate ERK 1/2 by dephosphorylating its phospho-serine/threonine and phospho-tyrosine residues hence regulating cell proliferation. [1]
- Interestingly however, current research postulates the non-specific function of DUSP6, acting as a tumour suppressor in pancreatic cancer, non-small cell lung cancer and ovarian cancer but having oncogenic properties in glioblastomas and thyroid carcinoma. [2]
- Due to the limited research done in associating DUSP6 mediated ERK regulation in colorectal carcinogenesis, this project aims to:
 - To quantify the expression of DUSP6, ERK and phospho-ERK (pERK) based on histopathological architecture and grade of dysplasia.
 - To compare DUSP6 expression with that of ERK and pERK to formulate a rationale for its function

Methodology

Immunohistochemistry staining for DUSP6, pERK and ERK were performed on colorectal adenomas, adenocarcinomas and normal cases (N=147), shown in Figure 1. (Image courtesy of Nourjahan Khafaga). Patient characteristics in the case cohort is denoted in Figure 2. (Left indicates from cecum up to hepatic flexure, Right indicates from descending colon up to rectum).

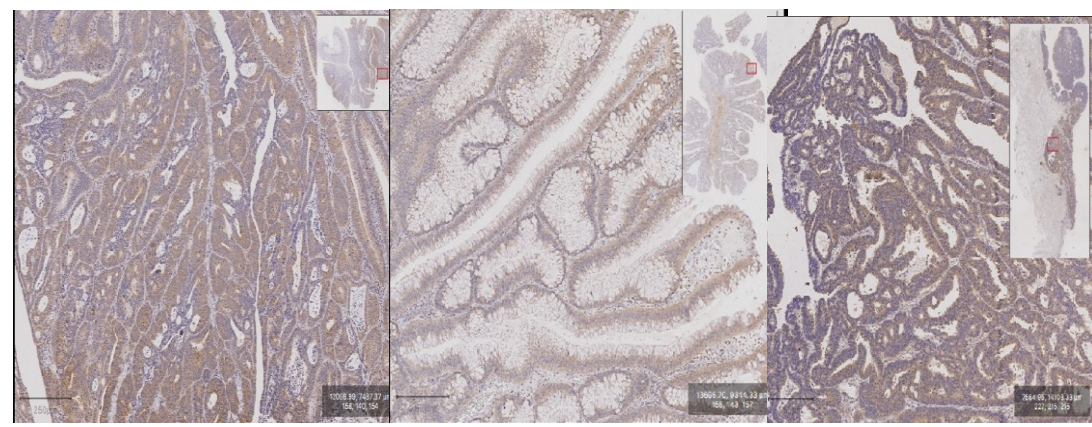


Figure 1 High staining intensity of DUSP6 in high grade dysplasia, villous adenoma and TP 53 respectively

	Number of Cases	Age at diagnosis, median (range)	Sex	Location
Normal Tissue (wildtype RAS and RAF)	15	66 (4-82)	10 Male, 5 Female	5 Right, 10 Left
Serrated Adenoma	10	70 (36-95)	8 Male, 2 Female	7 Right, 3 Left
Tubular Adenoma	25	63 (47-86)	12 Male, 13 Female	7 Right, 18 Left
Tubulovillous adenoma	33	67 (42-85)	23 Male, 10 Female	5 Right, 28 Left
Villous adenoma	19	63 (48-89)	11 Male, 8 Female	4 Right, 15 Left
Deficient Mismatch Repair Adenocarcinoma	15	71 (44-84)	1 Male, 14 Female	14 Right, 1 Left
KRAS Mutant Adenocarcinoma	15	53 (32-70)	6 Male, 9 Female	5 Right, 10 Left
TP53 Mutant Adenocarcinoma	15	65 (54-87)	6 Male, 9 Female	14 Right, 1 Left

Figure 2

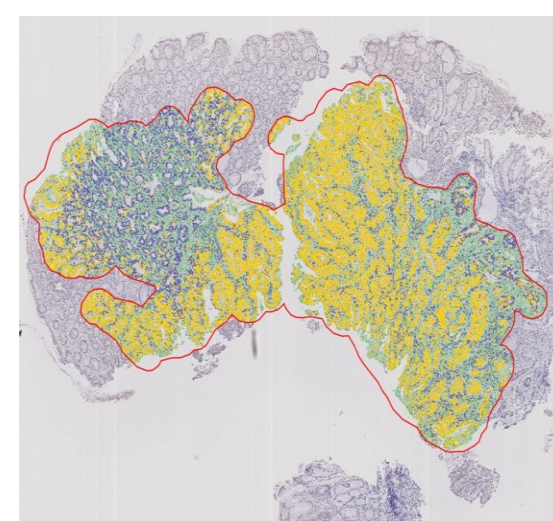


Figure 3

Conclusion

- Upregulated DUSP6 expression in high grade dysplasia and downregulation in majority of adenocarcinomas class is also seen in pancreatic cancers suggesting a tumour suppressive role. [3]
- Ratio of pERK : nuclear DUSP6 in high grade dysplasia suggests the upregulation of DUSP6, leading to dephosphorylation of pERK to suppress further cell proliferation.
- Loss of tumour suppressive functions of DUSP6 despite its high levels in TP53 mutant adenocarcinoma could be attributed to loss of cellular senescence programming allowing for the progression into this cancer class. [4]
- Deviation of serrated adenomas from other adenoma classes in terms of protein marker expressions aligns with the concept that they are of a molecularly distinct development pathway, i.e the serrated pathway compared with traditional adenomas that follow the typical adenoma-carcinoma sequence. [5]

Results

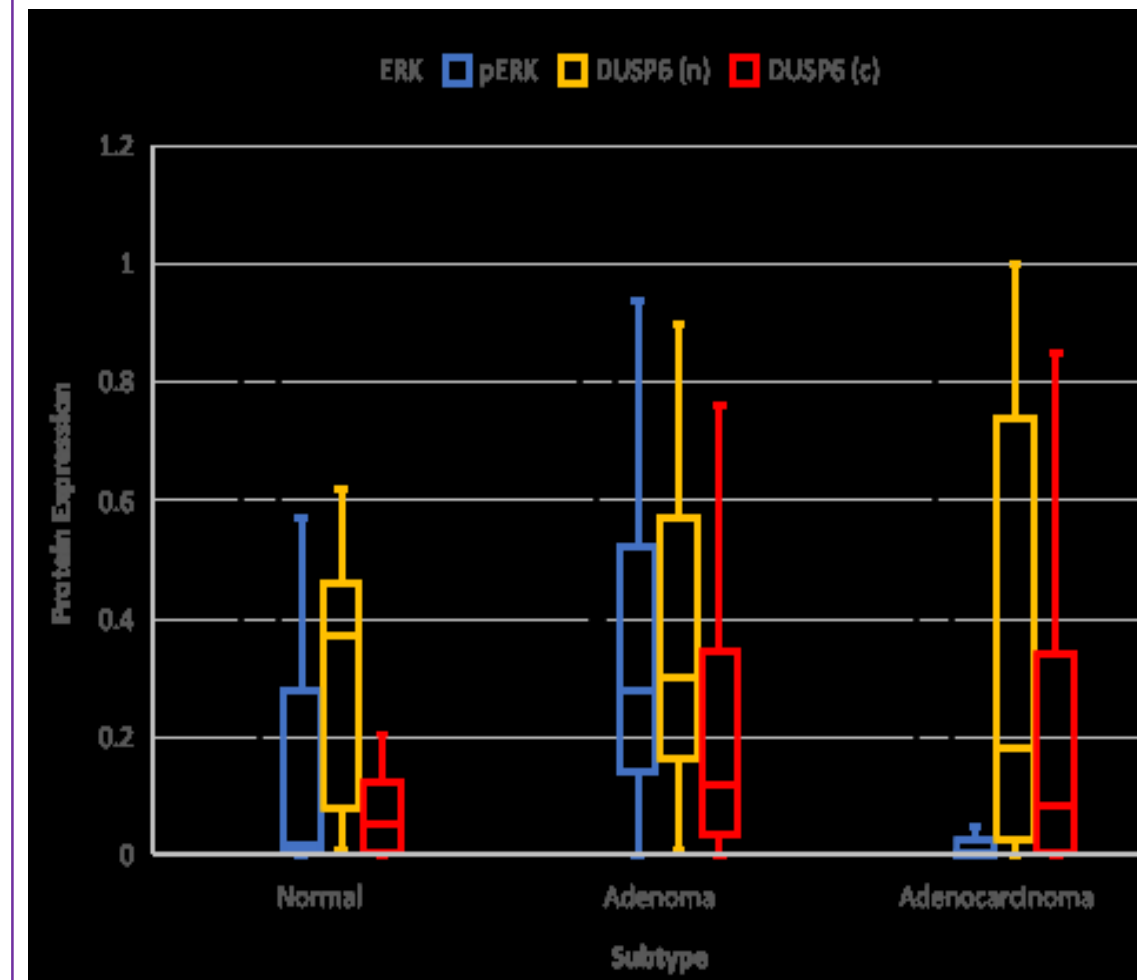


Figure 4. Box and whisker plot showing significantly greater nuclear DUSP6 expression compared to cytoplasmic DUSP6 within groups. (Wilcoxon signed rank, Monte Carlo adjustment). ERK expression significantly higher than pERK across groups (Kruskal Wallis test $p < 0.001$)

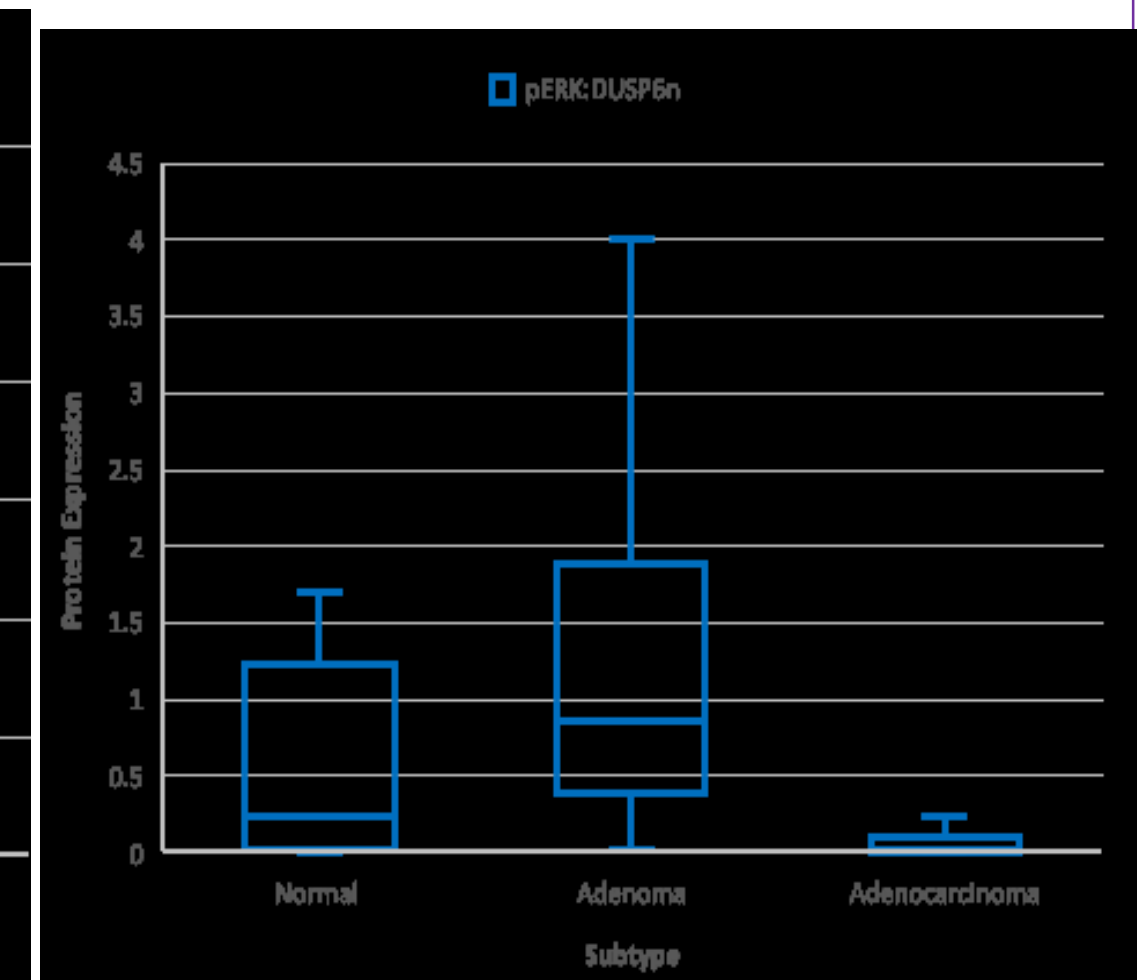


Figure 5. Ratio of pERK: nuclear DUSP6 expression in adenoma significantly higher than adenocarcinoma ($p < 0.001$) in plotted box and whisker plot

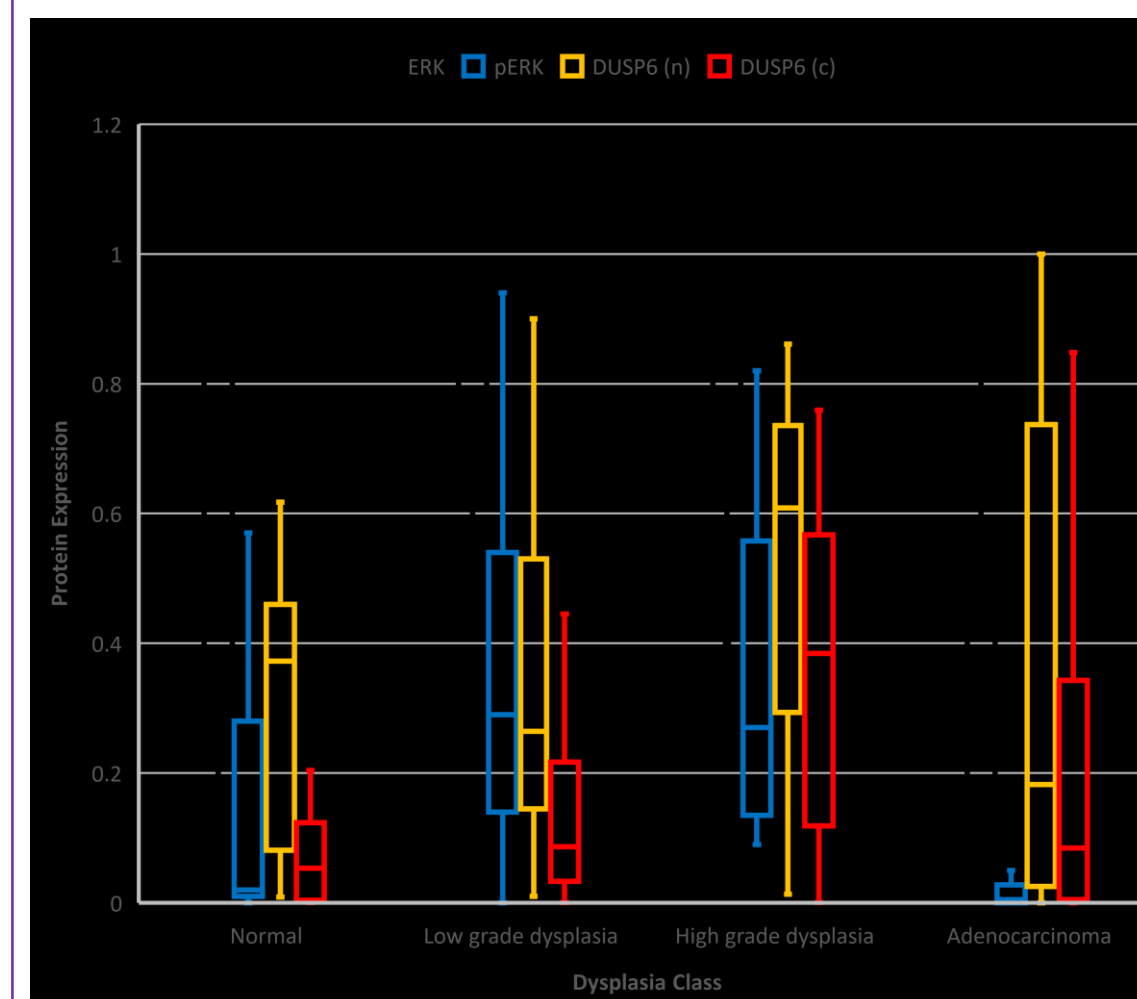


Figure 6. Significant difference between nuclear DUSP6 and cytoplasmic DUSP6 levels across dysplasia classes (Kruskal-Wallis test, $p < 0.009$ for nuclear DUSP6 and $p < 0.001$ for cytoplasmic DUSP6). ERK and pERK expression significantly higher for low and high grade dysplasia compared to normal and adenocarcinoma class.

Figure 7. Ratio higher at low grade dysplasia compared to high grade dysplasia and adenocarcinoma, where $p < 0.001$

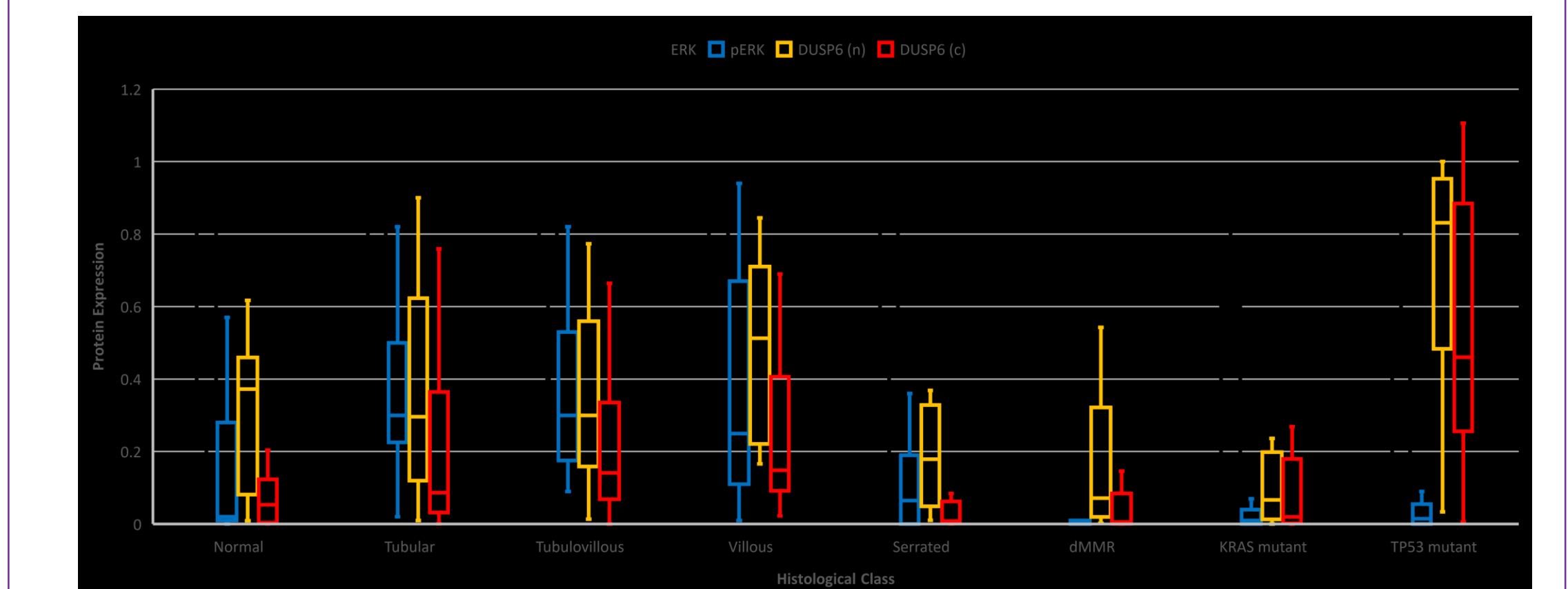


Figure 8. Significant difference between nuclear DUSP6 and cytoplasmic DUSP6 across histological classes (Kruskal-Wallis test, $p < 0.001$ for nuclear DUSP6 and $p < 0.001$ for cytoplasmic DUSP6). ERK and pERK higher for normal and adenomatous class than adenocarcinoma (Mann-Whitney test, Bonferroni adjustment $p < 0.001$)

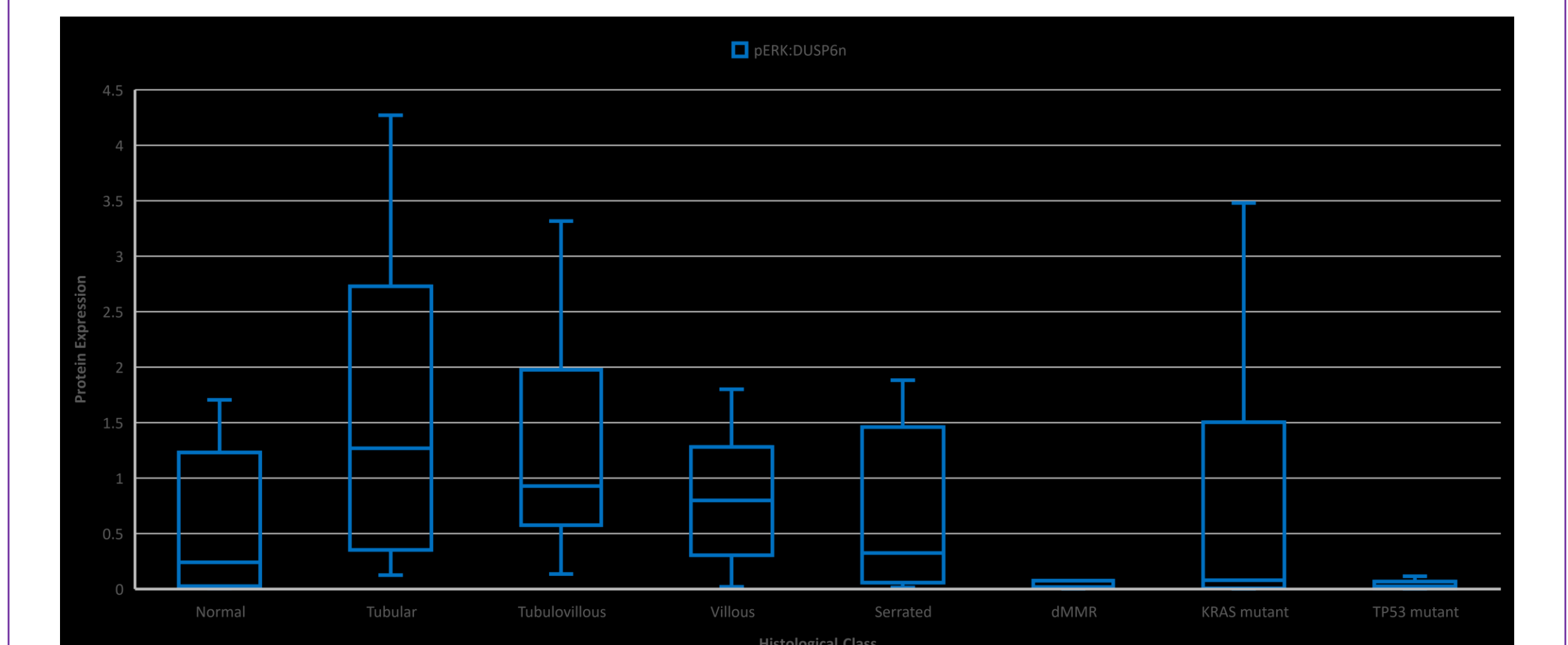


Figure 9. In adenoma class, ratio decreases from tubular, tubulovillous, villous to serrated adenoma mirroring the aggressive nature of the adenomas. dMMR and TP 53 mutants are significantly lower than adenoma class, $p < 0.001$.

References:
 1. Ncbi.nlm.nih.gov. (2018). *DUSP6 dual specificity phosphatase 6 [Homo sapiens (human)] - Gene - NCBI*. [online]
 2. Muhammad, K., Nur, A., Nurul, H., Narazah, M. and Siti, R. (2018). Dual-specificity phosphatase 6 (DUSP6): a review of its molecular characteristics and clinical relevance in cancer. *Cancer Biology & Medicine*, 15(1), p.14.
 3. Furukawa, T., Sunamura, M., Motoi, F., Matsuno, S. and Horii, A. (2003). Potential Tumor Suppressive Pathway Involving DUSP6/MKP-3 in Pancreatic Cancer. *The American Journal of Pathology*, 162(6), pp.1807-1815
 4. Fazeli, A., Steen, R., Dickinson, S., Bautista, D., Dietrich, W., Bronson, R., Bresalier, R., Lander, E., Costa, J. and Weinberg, R. (1997). Effects of p53 mutations on apoptosis in mouse intestinal and human colonic adenomas. *Proceedings of the National Academy of Sciences*, 94(19), pp.10199-10204.
 5. Patai, A. (2013). Serrated pathway: Alternative route to colorectal cancer. *World Journal of Gastroenterology*, 19(5), p.607.

